POLITECNICO DI TORINO

I Facoltà di Ingegneria
Corso di Laurea Specialistica in Ingegneria Meccanica

Tesi di Laurea

Numerical simulation of turbulent reactive flows

Relatori:
prof. Pietro Asinari
prof. Farzad Mashayek

Candidato:
Silvano Pautasso

Dicembre 2010

Ai miei genitori
(To my parents)

"The only source of knowledge is experience."

Albert Einstein

Acknowledgements

To begin, I would like to thank the most knowledgeable and helpful advisors, Prof. Pietro Asinari and Prof. Farzad Mashayek. If it wasn't for them I would not have the opportunity to spend these past few months at the University of Illinois at Chicago. My experience here has been unforgettable.

I would also like to thank the staff of the Department of Mechanical and Industrial Engineering of UIC for helping me whenever I needed, and my labmates of the *Computational Multiphase Transport Laboratory*: Harish, Karima, Hessam, and Ali. I would not have been able to come this far without their help. It was alway interesting and motivating to work with their company.

And finally, thank to my parents, who provide the unconditional support and love during all my university adventure.

Silvano Pautasso

Chicago, Illinois USA November 23, 2010

Summary

In this thesis reactive flow CFD (Computational Fluid Dynamics) simulations have been done with OpenFOAM. This work belongs to a long term research program of Prof. Mashayek. The program focuses on the turbulent reacting flow in combustion devices, which apply microjets as means of active control to improve combustion performance.

Nowadays many commercial CFD software packages are available. However, they do not allow one to costomize the code, and a such advanced topic as turbulent combustion become difficult to handle. For this reason, normally researchers need to develop their own code.

OpenFOAM is an open-source C++ toolbox. It is supplied with numerous preconfigured solvers, utilities, and libraries, so can be used like any typical simulation package. However, it is open-source therefore it is possible modify the code in function of any necessity;

In this thesis the capabilities of some preconfigured OpenFOAM solvers are tested. A comparison of a laminar fully premixed flame and a laminar partially premixed flame, with the study by B.Fiorina et al [2] was done. This work also presents a study of a turbulent reactive flow compared with Fuent results by Kanchi et al. [16] and experimental data Gould et al [15].

This work should be considered the first step to handle large reaction mechanisms and turbulence combustion with OpenFOAM.

Silvano Pautasso

Chicago, Illinois USA November 23, 2010

Contents

List of Tables

List of Figures

Part I

Chapter 1

Introduction

1.1 Motivation

This thesis is part of a long term research program focused on the turbulent reacting flow in combustion devices, which apply microjets as means of active control to improve combustion performance.

Combustion remains a key technology for the foreseeable future. It is therefore important to understand the mechanisms of combustion and, in particular, the role of turbulence within this process. In technical processes, combustion nearly always takes place within a turbulent rather than a laminar flow field for two reasons: turbulence increases the mixing process and enhances combustion, but at the same time combustion releases heat which generates flow instability through buoyancy, thus enhancing the transition to turbulence.

Turbulent combustion is still an open field of research. Turbulence itself is far from being fully understood; it's probably the most significant unresolved problem in classical physics. Turbulence models use systematic mathematical derivations based on Navier-Stokes equations up to a certain point, but then they introduce closure hypotheses which rely on dimensional arguments and require empirical input. Turbulence modeling is a huge research sector, but it is simply playing around without a breakthrough so far.

The apparent success of turbulence models in solving engineering flows has encouraged similar approaches for turbulent combustion, which has consequently led to the formulation of turbulent combustion models.

This thesis is the continuation of a previous work by Antonio Prochilo [1] were a solver for single-step reaction laminar reacting flows in OpenFOAM has been created. In order to go forward with this projet, we decide to use **large chemical mechanisms** in laminar cases, and **turbulent flows** in **dump combustor**.

1.2 What is CFD?

Flows and related phenomena can be described by partial differential (or integro-differential) equations, which cannot be solved analytically except in special cases. To obtain an approximate solution numerically, we have to use a *discretization method* which approximates the differential equations by a system of algebraic equations, which can then be solved on a computer. The approximations are applied to small domains in space and/or time so the numerical solution provides results at discrete locations in space and time. Much as the accuracy of experimental data depends on the quality of the tools used, the accuracy of numerical solutions is dependent on the quality of discretizations used. Contained within the broad field of computational fluid dynamics are activities that cover the range from the automation of well-established engineering design methods to the use of detailed solutions of the Navier-Stokes equations as substitutes for experimental research into the nature of complex flows. CFD can be very costs in term of time consuming, there are codes that may require hundreds of hours on the largest super-computers. CFD is finding its way into process, chemical, civil, and environmental engineering. Optimization in these areas can produce large savings in equipment and energy costs and in reduction of environmental pollution.

1.3 OpenFOAM

The OpenFOAM (Open Field Operation and Manipulation) CFD Toolbox can simulate anything from complex fluid flows involving chemical reactions, turbulence and heat transfer, to solid dynamics, electromagnetic and the pricing of financial options.

OpenFOAM is produced by OpenCFD Ltd, is freely available and open source, licensed under the GNU General Public Licence. The core technology of OpenFOAM is a flexible set of efficient C++ modules. These are used to build a wealth of:

- Solvers, to simulate specific problems in engineering mechanics;
- Utilities, to perform pre- and post-processing tasks ranging from simple data manipulations to visualization and mesh processing;
- Libraries, to create toolboxes that are accessible to the solvers/utilities, such as libraries of physical models.

OpenFOAM is supplied with numerous pre-configured solvers, utilities and libraries and so can be used like any typical simulation package. However, it is open, not only in terms of source code, but also in its structure and hierarchical design, so that its solvers, utilities and libraries are fully extensible.

OpenFOAM uses finite volume numerics to solve systems of partial differential equations ascribed on any 3D unstructured mesh of polyhedral cells.

Domain decomposition parallelism is fundamental to the design of OpenFOAM and integrated at a low level so that solvers can generally be developed without the need for any *"parallel-specific"* coding[8].

1.3.1 Sorver employed

In OpenFOAM some combustion solver are already present and we decide to use:

- reactingFoam (OF-1.7)
- alternateReactingFoam (OF-1.5)

reactingFoam is basically the simplest one and it is also can be used to simulate premixed and non-premixed flames.

alternateReactingFoam is very similar to reactingFoam with the exception of the chemistry package. Indeed, in reactingFoam the thermophysical propieties and the ODEs solver are implemented in OpenFOAM it self. Whereas, in alternateReactingFoam, through a library called *Alternate Chemistry Library*, uses Cantera[1] to implements the species propierties and it also solves the ODEs system using the CVODEs solver.

The reasons that the Alternate Chemistry Library has been created was that in OpenFOAM 1.5 the combustion model had many problems and bugs. Also the ODEs solver in OpenFOAM 1.5 is not very stable. Therefore, the aim of using alternateReactingFoam is to skip the combustion model of OpenFOAM and solve the chemistry package with Cantera. Even though the solver is much stable it still presents some problems:

- The library to interface OpenFOAM with Cantera works just with the version 1.5 of OpenFOAM, which still has many bugs.
- Cantera actually allows to have an easy access to thermochemical data and functions, but it has its own data structures for data about the species. These are not converted to OpenFOAM. The alternateSolver only needs and gets the mixture properties. Accessing other species properties involves heavy casting and specializing for the actually used chemistry implementation.
- The installation of the library is very tricky, especially on a multiprocessor machine.

[1]Cantera is a suite of object-oriented software tools for problems involving chemical kinetics, thermodynamics, and/or transport processes[18, 19].

For these reasons, we decided to stop using alternateReactingFoam. Thus this work will show only the results obtain with reactingFoam (OF-1.7). Though some test cases of alternateReactingFoam are present in the annexes.

1.4 Outline and contributions

This thesis should be considered the first approach to large reactions mechanisms and turbulence combustion. Starting from the results of this work some improvement can be done, especially in the conbustion model.

The main contributions of this thesis can be summarized as follows:

- To show how large reaction mechanisms are implemented and solved in OpenFOAM;
- To explain how to set up a turbulent combustion model in OpenFOAM;
- To study a premixed and a partially premixed laminar burner flame;
- To study the cold and reacting turbulent flow in an axisymmetric dump combustor;

The organization of the thesis will adhere to the following format: Chapter 2 reports a general form of the governing equations for gaseous laminar reacting flow. Chapter 3 reports the turbulent model governing equations. Chapter 4 describes the laminar test cases and the OpenFOAM pare- and post-processing. Chapter 5 describes the the study of the turbulent combustion in an dump combustor.

Chapter 2

Governing equations for laminar reacting flows

2.1 General form

In this chapter are described the equations which govern a laminar reactant flow. The derivation of these equations may be found in such standard book as the one by Williams [4].

2.1.1 Continuity equation

The continuity equation (scalar) is unchanged compared to non reacting-flow because combustion does not generate mass.

$$\frac{\partial \rho}{\partial t} + \nabla \cdot (\rho \mathbf{u}) = 0 \tag{2.1}$$

ρ is the density of the mixture[1], and $\mathbf{u}$ is the velocity field.

2.1.2 Species equations

For a mixture of N species, the (scalar) equation for the specie k is [2]:

$$\frac{\partial \rho Y_k}{\partial t} + \nabla \cdot (\rho \left(\mathbf{u} + \mathbf{V}_k\right) Y_k) = \dot{\omega}_k \quad \text{for} \quad k = 1,N \tag{2.2}$$

where $\mathbf{V}_k$ is the diffusion velocity of species k, and $\dot{\omega}_k$ is the reaction rate of species k. The equation. 2.2 is solved for N-1 species. Since the mass fraction of the species

[1] $\rho = \sum_{k=1}^{N} \rho_k$

[2] $Y_k = \frac{m_k}{m}$ where m_k is the mass of the species k, and m is the total mass of the mixture.

must sum to unity, so for the N_{th} mass fraction is determined as one minus the sum of the N-1 solved mass fractions.

2.1.3 Momentum equation

The momentum equation for the gas reads

$$\frac{\partial \rho \mathbf{u}}{\partial t} + \nabla \cdot (\rho \mathbf{u} \otimes \mathbf{u} + p\mathbf{I}) = \nabla \cdot \mathbf{\Pi}_\nu + \rho \sum_{k=1}^{N} Y_k \mathbf{f}_k + \rho \mathbf{g} \tag{2.3}$$

where $\mathbf{f}_k$ is the volume force acting on species k, and $\mathbf{g}$ is the gravity acceleration and $\mathbf{\Pi}_\nu$ is the viscous stress tensor. Even though this equation does not include explicit reaction terms, the flow is modified by combustion because both the dynamic viscosity μ and the density ρ are functions of temperature.

2.1.4 Total energy equation

The energy equation (a scalar equation) requires the greatest attention because multiple forms exist. The equation for the total energy e_t (sensible + kinetic + chemical) is:

$$\frac{\partial \rho e_t}{\partial t} + \nabla \cdot (\rho \mathbf{u} e_t + p\mathbf{u}) = \nabla \cdot (-\mathbf{q} + \mathbf{\Pi}_\nu \mathbf{u}) + \dot{Q} + \rho \sum_{k=1}^{N} Y_k \mathbf{f}_k (\mathbf{u} + \mathbf{V}_k) \tag{2.4}$$

where $\dot{Q}$ is the heat source term (due, for example, to an electric spark, a laser, or radiative flux), and should not to be confused with the heat released by combustion. The flux $\mathbf{q}$ includes a heat diffusion term (which can be expressed by Fourier's law) and a second term, which is specific of multi-species gas, is associated with the diffusion of species with different enthalpies.

$$\mathbf{q} = \mathbf{q}_\alpha + \rho \sum_{k=1}^{N} h_k Y_k \mathbf{V}_k. \tag{2.5}$$

Subtracting the term $\frac{1}{2}\mathbf{u} \otimes \mathbf{u}$ from the equation (2.4) we get the balance equation for e (sensible+chemical energy):

$$\frac{\partial \rho e}{\partial t} + \nabla \cdot (\rho \mathbf{u} e + p\mathbf{u}) = \nabla \cdot (-\mathbf{q} + \mathbf{\Pi}_\nu \mathbf{u}) + \dot{Q} + \rho \sum_{k=1}^{N} Y_k \mathbf{f}_k \mathbf{V}_k \tag{2.6}$$

Form	Energy	Enthalpy
Sensible	$e_s = \int_{T_0}^{T} c_v dt - RT_0/W$	$h_s = \int_{T_0}^{T} c_p dt$
Sensible+Chemical	$e = e_s + \sum_{k=1}^{N} \Delta h^0_{f,k} Y_k$	$h = h_s + \sum_{k=1}^{N} \Delta h^0_{f,k} Y_k$
Total Chemical	$e_t = e + \frac{1}{2}\mathbf{u} \otimes \mathbf{u}$	$h_t = h + \frac{1}{2}\mathbf{u} \otimes \mathbf{u}$
Total non Chemical	$E = e_s + \frac{1}{2}\mathbf{u} \otimes \mathbf{u}$	$H = h_s + \frac{1}{2}\mathbf{u} \otimes \mathbf{u}$

Table 2.1: Enthalpy and energy forms used in conservation equations

2.1.5 Enthalpy equation

Using the relation between energy and enthalpy: $h = e + p/\rho$ and the continuity equation 2.1 yields:

$$\rho \frac{De}{Dt} = \frac{\partial \rho e}{\partial t} + \nabla \cdot (\rho \mathbf{u} e) = \rho \frac{Dh}{Dt} - \frac{Dp}{Dt} - \nabla \cdot (p\mathbf{u}) \tag{2.7}$$

the conservation equation for enthalpy h can be deduced from the equation (2.6):

$$\frac{\partial \rho h}{\partial t} + \nabla \cdot (\rho \mathbf{u} h) = \frac{Dp}{Dt} - \nabla \cdot \mathbf{q} + \mathbf{\Pi}_\nu \mathbf{:} \nabla \mathbf{u} + \dot{Q} + \rho \sum_{k=1}^{N} Y_k \mathbf{f}_k \mathbf{V}_k. \tag{2.8}$$

From the definition of h_s (tab. 2.1), substituting h_s for h in the (2.8) leads to the sensible enthalpy equation

$$\frac{\partial \rho h_s}{\partial t} + \nabla \cdot (\rho \mathbf{u} h_s) = \dot{\omega}_T + \frac{Dp}{Dt} - \nabla \cdot \mathbf{q} + \mathbf{\Pi}_\nu \mathbf{:} \nabla u + \dot{Q} + \rho \sum_{k=1}^{N} Y_k \mathbf{f}_k \mathbf{V}_k. \tag{2.9}$$

where $\dot{\omega}_T = \sum_{k=1}^{N} \Delta h^0_{f,k} Y_k \dot{\omega}_k$

2.2 Constitutive relations

In order to close the system, it is necessary to introduce additional, so-called constitutive relations. They depend on the properties of the continuous medium in question. The following set is used:

2.2.1 Stokes closure

For the viscous stress tensor $\mathbf{\Pi}_\nu$, the generalized form of the Newton's law of viscosity is used:

$$\mathbf{\Pi}_\nu = \rho\nu \left(\nabla \mathbf{u} + \nabla \mathbf{u}^T \right) + \rho \left(\nu_B - 2/3\nu \right) \nabla \cdot \mathbf{u} \mathbf{I} \tag{2.10}$$

where:

- ν is the kinematic viscosity [3] [m^2/s];
- ν_B is the bulk kinematic viscosity [m^2/s];

2.2.2 Fourier closure

The heat diffusion flux is expressed by using the Fourier's law of heat conduction:

$$\boldsymbol{q} = \mathbf{q}_\alpha + \sum_{k=1}^{N} h_{s,k} Y_k \mathbf{V}_k \tag{2.11}$$

with

$$\boldsymbol{q}_\alpha = -\lambda \nabla T = -\alpha \rho c_p \nabla T \tag{2.12}$$

- λ is the thermal conductivity [W/mK];
- $\alpha = \dfrac{\lambda}{\rho c_p}$ is the thermal diffusivity [m^2/s];

2.2.3 Diffusion velocities

The molecular transport processes that cause the diffusive fluxes are quite complicated. A full description may be found in Williams (1985) [4]. Since in model of turbulent combustion molecular transport is less important than turbulent transport, it is useful to consider simplified versions of the diffusive fluxes; the most elementary is the binary flux approximation [3]

$$\mathbf{V}_k = -D_k \nabla Y_k \tag{2.13}$$

where D_k is the binary diffusion coefficient, or mass diffusivity, of species k with respect to an abundant specie, for instance N_2.

2.3 Consideration and simplification

2.3.1 Mass fractions equation

OpenFOAM assumes the unity Lewis number [4] for all the species in order to simplify the mass fraction equation. Thus, according to this assumption, the equation (2.2)

[3] $\nu = \dfrac{\mu}{\rho}$, μ is the dynamic viscosity.

[4] $Le = \dfrac{\alpha}{D_k}$

becomes

$$\rho\frac{\partial Y_k}{\partial t} + \nabla\cdot(\rho\boldsymbol{u}Y_k) = \nabla\cdot(\mu\nabla Y_k) + \dot{\omega}_k \tag{2.14}$$

As we told before this equation is solved N-1 times: indeed, for the N_{th} specie (in our case is N_2 which is also the inert one) the mass fraction is calculated subtracting the sun of all the others Y_k to one

$$Y_{N_2} = 1 - \sum_{k=1}^{N-1} Y_k \tag{2.15}$$

which means that all the mass errors are accumulated in the term Y_{N_2}.

2.3.2 Enthalpy equation in OpenFOAM

In the previous versions of OpenFOAM (ver 1.5 and 1.6) a total enthalpy equation is solved, while the last version (ver.1.7) solves a sensible enthalpy equation. Let's make some consideration about some terms of these two equations:

Dp/Dt This term is negligible in open flames, where $p \approx constant$. It should be retained in case of reciprocating engines for example. This effect is accounted in reactingFoam.

$\Pi_\nu : \nabla\mathbf{u}$ This represents the viscous (or frictional) heating. Here, $(:)$ represents the inner product of tensors. This term is negligible for low-speed flows and is *not* considered in reactingFoam.

$\dot{Q}$ By default, there is not a heat source term, therefore it is neglected. However, it is possible to add a sub-application to create a spark which basically adds this term to the equation.

$\sum_{k=1}^{N} Y_k\mathbf{f}_k\mathbf{V}_k$ For most cases body forces are zero ($\boldsymbol{f}_k = 0$), therefore all the term becomes null.

Neglecting the terms not solved in reactingFoam the total ehntalpy equation (2.8) becomes

$$\frac{\partial(\rho h)}{\partial t} + \nabla\cdot(\rho\boldsymbol{u}h) = \nabla\cdot(\lambda\nabla T) + \nabla\cdot\sum_{k=1}^{N_s}(h_k\rho D_k\nabla Y_k) + \frac{Dp}{Dt} \tag{2.16}$$

and if we write the term containing T in terms of h, with some further algebric steps we get

$$\frac{\partial(\rho h)}{\partial t} + \nabla \cdot (\rho \boldsymbol{u} h) = \nabla \cdot (\rho \alpha \nabla h) + \nabla \cdot \sum_{i=1}^{N_s} \left[(h_k \nabla Y_k) (\rho D_k - \rho \alpha) \right] + \frac{Dp}{Dt}. \quad (2.17)$$

In OpenFOAM 1.5 and 1.6 also for the enthalpy equation the unity Levis number is assumed, thus all the sommation in the above equation goes to zero, and finally the equation solved in the solver is:

$$\frac{\partial(\rho h)}{\partial t} + \nabla \cdot (\rho \boldsymbol{u} h) = \nabla \cdot (\rho \alpha \nabla h) + \frac{Dp}{Dt}. \quad (2.18)$$

While for the sensible entalpy the term $\nabla \cdot \sum_{k=1}^{N} h_{s,k} Y_k \mathbf{V}_k$ is zero:

- if the mixture contains only one specie or
- if all the species have the same sensible enthalpy

in all the other cases, this tern does not vanish even though it is sometimes set to zero it is usually negligiable compared to $\dot{\omega}_T$ (reactingFOAM makes this hypotehsis). Thus the h_s equation in OpenFOAM 1.7 is:

$$\frac{\partial \rho h_s}{\partial t} + \nabla \cdot (\rho \mathbf{u} h_s) = \dot{\omega}_T + \frac{Dp}{Dt} + \nabla \cdot (\rho \alpha \nabla hs) \quad (2.19)$$

2.4 Chemistry and thermophysichal properties

2.4.1 Chemistry

OpenFoam can handle big reaction mechanisms which involves many elementary steps and many species. Solving the chemistry numerically means solving a large system of reaction equations. For each reaction[14]

$$S_{11}^f [X_1] + S_{21}^f [X_2] + \cdots \rightarrow S_{11}^r [X_1] + S_{21}^r [X_2] + \cdots \quad (2.20)$$

there is a corresponding reaction rate equation which determines how rapidly the reaction is proceeding and in which direction. To formulate the reaction in a more general manner, reaction j is written as:

$$\sum_{k=1}^{N_s} S_{kj}^f [X_k] \rightleftharpoons_{k_j^r}^{k_j^f} \sum_{k=1}^{N_s} S_{kj}^r [X_k] \quad (2.21)$$

where S^f and S^r are the matrices of forward and reverse stoichiometric coefficients, respectively, k_j^f and k_j^r are the corresponding reaction rate constants of reaction j, and $[X_k]$ is the molar concentration of the k_{th} species in the cell. The stoichiometric coefficients' matrix has N_s rows, with the rows corresponding to species. The columns represent reactions, making the matrix $N_s \times N_r$. The reaction rate k is itself a function of the Arrhenius constants:

$$k(T) = AT^b exp(-\frac{E_a}{R_u T}) \tag{2.22}$$

which need to be specified as part of the mechanism. It is now possible to write the equation for the reaction rate of the basic reaction (2.20). The rate of formation of species $[X_1]$ from reaction j is written as

$$\left(\frac{d[X_1]}{dt}\right)_j = S_{1j}^r \left(k_j^f \prod_{k=1}^{N_s} [X_k]^{S_{1j}^f} - k_j^r \prod_{k=1}^{N_s} [X_k]^{S_{1j}^r}\right) \tag{2.23}$$

This equation is formulated for every species included in the chemical mechanism, as well as for every reaction, resulting in an equation system consisting of $N_s \times N_r$ equation. As can be seen from the above equation, it is a system of Ordinary Differential Equations (ODEs), which can be solved by an ODEs solver already integrated in OpenFOAM. Aside from the concentrations, it is also important to find the right hand side of equation (2.23). The source term for species k is:

$$\dot{\omega}_k = \frac{W_k}{\rho} \sum_j^{N_r} \left(S_{kj}^r - S_{kj}^f\right) \left(k_j^f \prod_{k=1}^{N_s} [X_k]^{S_{kj}^f} - k_j^r \prod_{k=1}^{N_s} [X_k]^{S_{kj}^r}\right). \tag{2.24}$$

In OpenFOAM the Arrhenius and stoichiometric coefficient are provide by the mechanism reaction file (Chemkin format). An example for one-step reaction mechanism for propane combustion is given below:

```
ELEMENTS
H O C N
END
SPECIE
O2 H2O   CO2  N2   C3H8
END
REACTIONS!                          A    b  Ea
C3H8 + 5O2 => 3CO2 + 4H2O       8.6E11  0 30000 !1
        FORD     / C3H8 0.1 /
        FORD     / O2   1.65 /
END
```

where the three numbers before the exclamation mark are A, β, and E_a of Arrhenius formula. The units for A are $(mol/cm^3)^{1-m-n}/s$ [5] and the activation energy is expressed in cal/mol.

2.4.2 Thermophysical properties

OpenFOAM is also able to read Chemkin thermo files which contain all information about species heatcapacity, enthalpy and entropy. These quantities are supplied using polynomials as follows:

$$\frac{C^{\circ}_{pk}}{R} = a_{1k} + a_{2k}T_k + a_{3k}T_k^2 + a_{4k}T_k^3 a_{5k}T_k^4 \tag{2.25}$$

$$\frac{H^{\circ}_{k}}{RT_k} = a_{1k} + \frac{a_{2k}}{2}T_k + \frac{a_{3k}}{3}T_k^2 + \frac{a_{4k}}{4}T_k^3 + \frac{a_{5k}}{5}T_k^4 + \frac{a_{6k}}{T_k} \tag{2.26}$$

$$\frac{S^{\circ}_{k}}{R} = a_{1k}\ln T_k + a_{2k}T_k + \frac{a_{3k}}{2}T_k^2 + \frac{a_{4k}}{2}T_k^3 + \frac{a_{5k}}{4}T_k^4 + a_{7k} \tag{2.27}$$

where $\circ$ means standard state based on pressure (in our case 1 atm), and R is the gas constant. An example of *Thermo.dat* file for the species of the above propane single-step reaction is showed below:

```
THERMO ALL
   200.000  1000.000  5000.000
C3H8             120186C   3H   8          G  0200.00   5000.00  1000.00      1
 0.07525217E+02 0.01889034E+00-0.06283924E-04 0.09179373E-08-0.04812410E-12    2
-0.01646455E+06-0.01784390E+03 0.08969208E+01 0.02668986E+00 0.05431425E-04    3
-0.02126001E-06 0.09243330E-10-0.01395492E+06 0.01935533E+03                   4

O2               121386O   2              G  0200.00   5000.00  1000.00      1
 0.03697578E+02 0.06135197E-02-0.01258842E-05 0.01775281E-09-0.01136435E-13    2
-0.01233930E+05 0.03189166E+02 0.03212936E+02 0.01127486E-01-0.05756150E-05    3
 0.01313877E-07-0.08768554E-11-0.01005249E+05 0.06034738E+02                   4

CO2              121286C   1O   2          G  0200.00   5000.00  1000.00      1
 0.04453623E+02 0.03140169E-01-0.01278411E-04 0.02393997E-08-0.01669033E-12    2
-0.04896696E+06-0.09553959E+01 0.02275725E+02 0.09922072E-01-0.01040911E-03    3
 0.06866687E-07-0.02117280E-10-0.04837314E+06 0.01018849E+03                   4

H2O               20387H   2O   1          G  0200.00   5000.00  1000.00      1
 0.02672146E+02 0.03056293E-01-0.08730260E-05 0.01200996E-08-0.06391618E-13    2
-0.02989921E+06 0.06862817E+02 0.03386842E+02 0.03474982E-01-0.06354696E-04    3
```

[5] m and n are the reaction exponents. In this example $m = 0.1$ and $n = 1.65$

```
 0.06968581E-07-0.02506588E-10-0.03020811E+06 0.02590233E+02                   4

N2                121286N   2               G  0200.00   5000.00  1000.00      1
 0.02926640E+02 0.01487977E-01-0.05684761E-05 0.01009704E-08-0.06753351E-13    2
-0.09227977E+04 0.05980528E+02 0.03298677E+02 0.01408240E-01-0.03963222E-04    3
 0.05641515E-07-0.02444855E-10-0.01020900E+05 0.03950372E+02                   4

END
```

Line number 2 includes the temperature ranges for two sets of coefficients describing the polynomials. The species name starts line number 3 where the elementary composition must also be declared as well as phase and temperature range. Lines number 4-6 represent the coefficients used in equations (2.25), (2.26) and (2.27) for two sets of temperature ranges.

2.4.3 Transport properties

The laminar dynamic viscosity μ in $Kg/(ms)$ is calculated using Sutherland's law where the constants A_s and T_s are hard coded in to OpenFOAM

$$\mu = A_s \frac{T^{1/2}}{1 + T_s/T} \tag{2.28}$$

while the thermal diffusivity α in turn is implemented from μ

$$\alpha = \mu C_v \left(1.32 + \frac{1.77R}{C_v}\right). \tag{2.29}$$

Chapter 3

Turbulent reacting flows

3.1 Introduction

The description of turbulent combustion processes using Computational Fluid Dynamics (CFD) may be achieved using three levels of computations

- Reynolds Average Navier Stokes (or RANS) computations was the first possible approach in the past because it demands less CPU efforts. Therefore, RANS techniques were developed to solve for the mean values of all quantities corresponding average quantities over time for stationary mean flows or average over different realization (or cycles) or periodic flows like those found in the pistons engine. For a stabilized flame, the temperature periodic with RANS at a given point is constant corresponding to the mean temperature at this point (Fig.3.1).

- The second level corresponds to Large Eddys Simulations(LES). In this approach the turbulence large scale are explicitly calculated while the subgrid closure rules are used to model the effect of the smaller ones. Thus LES determines the instantaneous position of a large scales but a subgrid model is still required to take in to account the effect of small turbulent scales on combustion. LES would capture the low-frequency variations of temperature (Fig.3.1).

- The last lever corresponds to Direct Numerical Simulation (DNS) where the full instantaneous Navier-Stokes equation are solved with out any model for turbulent motion. Also the turbulence small scales are directly solved, thus DNS can also predict high-frequency variations (fig.3.1).

In term of computer requirements, CFD for non-reacting and reacting flows follows similar trends: The DNS method is the most demanding one and it is limited

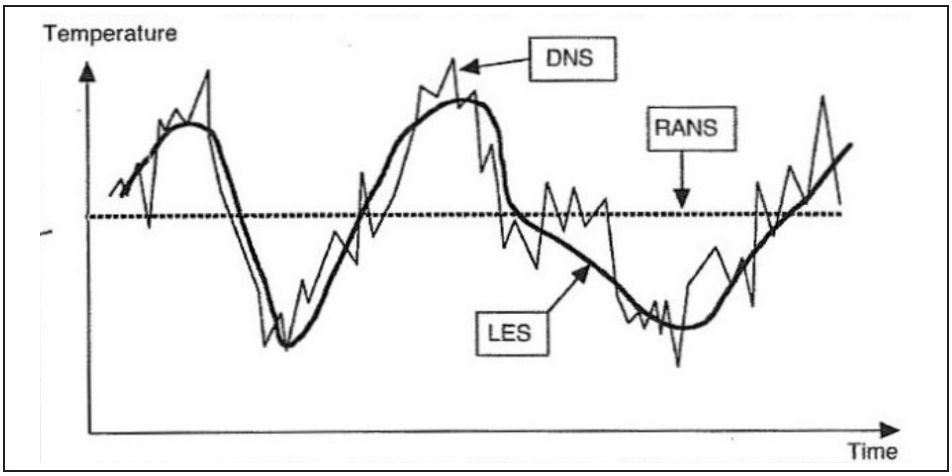

Figure 3.1: Time evolution for a local variable with RANS, LES or DNS. Source[9]

to small Reynolds numbers and simplified geometry. LES works with a coarser mesh (it has to resolve only large scale), and it is also able to handle higher Reynolds numbers but required sub-grid models. RANS is extensively used because it required less in terms of resources but this validity is limited by the closure models describing turbulence and combustion. A brief comparison between RANS, LES and DNS is summarized in table below

Approach	Advantages	Drawbacks
RANS	Coarse mesh Geometrical simplification (2D, symmetry,..) Reduced numerical costs	Only mean flow field Models required
LES	Unsteady features Reduced modelling impact (compared to RAS)	Models required 3D simulation required Needs precise codes Numerical costs
DNS	No models needed Tool to study models	Prohibitive numerical costs Limited to academics problems

Table 3.1: Comparison between RANS, LES and DNS [9].

In this work the RANS approach has been followed, in particular the *k-epsilon* model has been used.

3.2 K-epsilon model

The simplest models of turbulence are two-equation models in which the solution of two separate transport equations allows the turbulent velocity and length scales

to be independently determined and the $k-\epsilon$ model falls within this class of the turbulence model. It is a semi-empirical and based on model transport equations for the turbulence kinetic energy (k) and the dissipation rate (ϵ). Where the transport equation for k is derived from an exact equation while for ϵ the transport equation is obtained using physical reasoning and bears little resemblance to its mathematically exact counterpart. Furtheremore, in the $k-\epsilon$ model it is assumed that the flow is fully turbulent.

3.2.1 Transport equations for k and ϵ

The transport equations for k and ϵ for a compressible flow are:

$$\frac{\partial \rho k}{\partial t} + \nabla \cdot (\rho \mathbf{u} k) + \nabla \cdot \left(D_{k_{eff}} \nabla k\right) = G - \left(\frac{2}{3}\rho \nabla \cdot \mathbf{u}\right) k - \rho\epsilon \tag{3.1}$$

$$\frac{\partial \rho \epsilon}{\partial t} + \nabla \cdot (\rho \mathbf{u} \epsilon) + \nabla \cdot \left(D_{\epsilon_{eff}} \nabla \epsilon\right) = C_1 G \frac{\epsilon}{k} - \left[\left(\frac{2}{3}C_1 + C_3\right)\rho \nabla \cdot \mathbf{u}\right]\epsilon - C_2 \rho \frac{\epsilon^2}{k} \tag{3.2}$$

where:

- $G = (\mu_t \nabla \mathbf{u}) : \left[\left(\nabla \mathbf{u} + \nabla \mathbf{u}^T\right) - \nabla \cdot \mathbf{u}\mathbf{I}\right]$
- $D_{k_{eff}}$ is the effective diffusivity for k and $D_{k_{eff}} = \dfrac{\mu_t}{\sigma_k} + \mu_{lam}$
- $D_{\epsilon_{eff}}$ is the effective diffusivity for ϵ and $D_{\epsilon_{eff}} = \dfrac{\mu_t}{\sigma_\epsilon} + \mu_{lam}$
- C_1, C_2 C_3 are empirical constants

and

- σ_ϵ and σ_k are the turbulent Prandtl numbers for ϵ and k
- μ_t is the turbulent viscosity. $\mu_t = \rho C_\mu \dfrac{k^2}{\epsilon}$

the turbulent thermal diffusivity is calculated using a constant Prandtl number thus $\alpha_t = \dfrac{\mu_t}{Pr_t}$.

Typical values of the k-ϵ model coefficients are relate in table 3.2.1

Coeff.	value
C_μ	0.09
C_1	1.44
C_2	1.92
C_3	-0.33
σ_k	1.0
σ_k	1.3
Pr_t	1

Table 3.2: default values of k-ϵ model coefficients

3.2.2 Coupling k and ϵ with the Navier-Stoks equations

The two new variable k and ϵ basically are coupled with the Navier-Stoks equation thru the viscosity and the thermal diffusivity. Indeed they become:

$$\mu = \mu_{eff} = \mu_{lam} + \mu_t \tag{3.3}$$

$$\alpha = \alpha_{eff} = \alpha_{lam} + \alpha_t \tag{3.4}$$

where α_{lam} and μ_{lam} are the one calculated with the equations (2.28) and (2.29). Note that in a laminar case α_t and μ_t are egual to zero.

3.2.3 Chalmers PaSR-Model

It is necessary to use some form of treatment for the chemistry and turbulent mixing. In this work *Chalmers PaSR-Model* has been used. It is based on the theory that real flames are much thinner than any computational cell, so assuming that an entire cell is a perfect reactor is a severe overestimation. Thus, the cells are divided into a reacting part and a non-reacting part. The reacting part is treated like a perfectly stirred reactor in which all present species are homogeneously mixed and reacted. After reactions have taken place, the species are assumed to be mixed due to turbulence for the mixing time τ_{mix} and the resulting concentration gives the final concentration in the entire, partially-stirred, cell. The reaction rate term for species k is then approximated as[14]:

$$\frac{\partial c^k}{\partial t} = \frac{c_1^k - c_0^k}{\tau_c} = \kappa \dot{\omega_k} \tag{3.5}$$

where $\dot{\omega_k}\left(c_1^k\right)$ is the laminar chemical source term, and κ the reaction rate multiplier,

defined as:

$$\kappa = \frac{\tau_f + \tau_c}{\tau_f + \tau_c + \tau_{mix}} \tag{3.6}$$

where:

- τ_f is the flow time step and it just depends from the time set in `controlDict` file. Furthermore, it is much smaller than τ_c and τ_{mix} thus, it is usually negligible.
- τ_c is dependent on the reaction coefficients and temperature.
- τ_{mix} is defined as $\tau_{mix} = C_{mix}\sqrt{\frac{\mu_{eff}}{\rho\epsilon}}$ if μ_{lam} is considered negligible compared with μ_{tub} one can say that $\tau_{mix} = C_{mix}\sqrt{C_\mu}\frac{k}{\epsilon} = C'_{mix}\frac{k}{\epsilon}$. k over ϵ is the turbulence time scale. Thus, the coefficient C_{mix} links the turbulence time scale with the mixing one.

The reactive fraction κ appears in the species transport equation with the chemical source term as shown below:

$$\rho\frac{\partial Y_k}{\partial t} + \rho\boldsymbol{u}\cdot\nabla Y_k = \nabla\cdot(\rho\alpha\nabla Y_k) + \kappa\dot{\omega}_k \tag{3.7}$$

and also in the enthalpy equation:

$$\frac{\partial\rho h_s}{\partial t} + \nabla\cdot(\rho\mathbf{u}h_s) = \kappa\dot{\omega}_T + \frac{Dp}{Dt} + \nabla\cdot(\rho\alpha\nabla h_s) \tag{3.8}$$

Part II

Cases

Chapter 4

Laminar Cases

4.1 Introduction

In order to fully validate the code for laminar cases, numerical simulations have been performed for two-dimensional burner configurations:

- a fully premixed flame (case 1) and
- a partially premixed flame (case 2).

The simulation results have been compared with the publish research by Fiorina et al [2].

4.1.1 File structure

The structure of basic directories in OpenFOAM normally contain three main folders (figure 4.1):

- A `constant` folder contains some files where the physical properties of the fluid/species and the turbulence model are set. It also contain the sub-folder, `polyMesh`, which has the geometry and boundary condition patches for the mesh.
- The `system` folder that contains three files for setting various system specific properties are: `controlDict`, where run control parameters are set including start/end time, time step and parameters for data output; `fvSchemes`, where discretization schemes used in the solution may be selected; and `fvSolution`, where the equation solvers, tolerances, and other algorithm controls are set for the run.
- `time` folders contain the calculated properties, such as velocity, temperature, etc. The *0* folder is used to set the initials and boundary conditions.

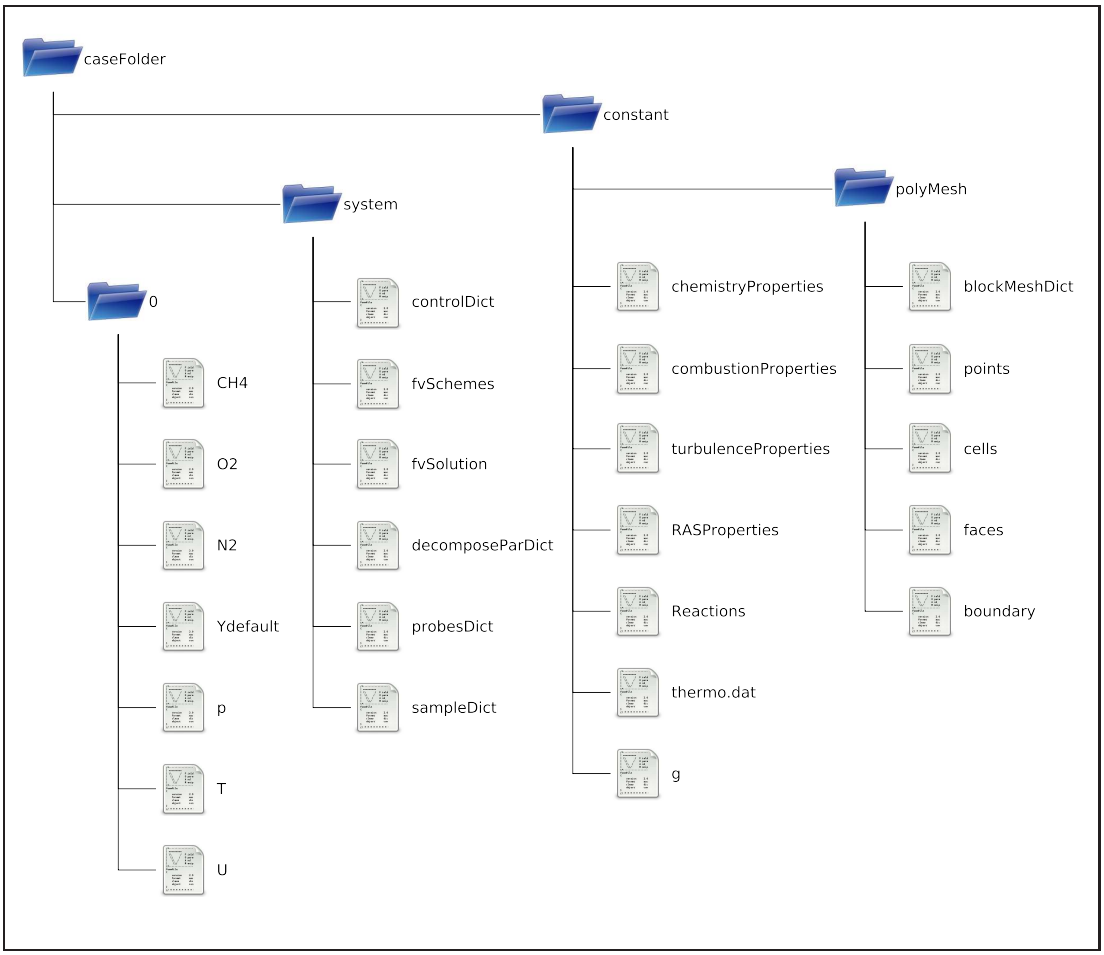

Figure 4.1: File structure for a reactingFOAM case using the RANSmodel

4.2 Preprocessing - case 1

This case corresponds to a fully premixed methane/air two-dimensional laminar burner studied in [2]. The configuration of the burner is shown in figure 4.2. The computation has been done for half of the domain because of the symmetry geometry of the burner.

4.2.1 Regime flow

In order to make sure that we are dealing with a laminar flow, we calculated the Reynolds number which is one of the most frequently used dimensionless parameter

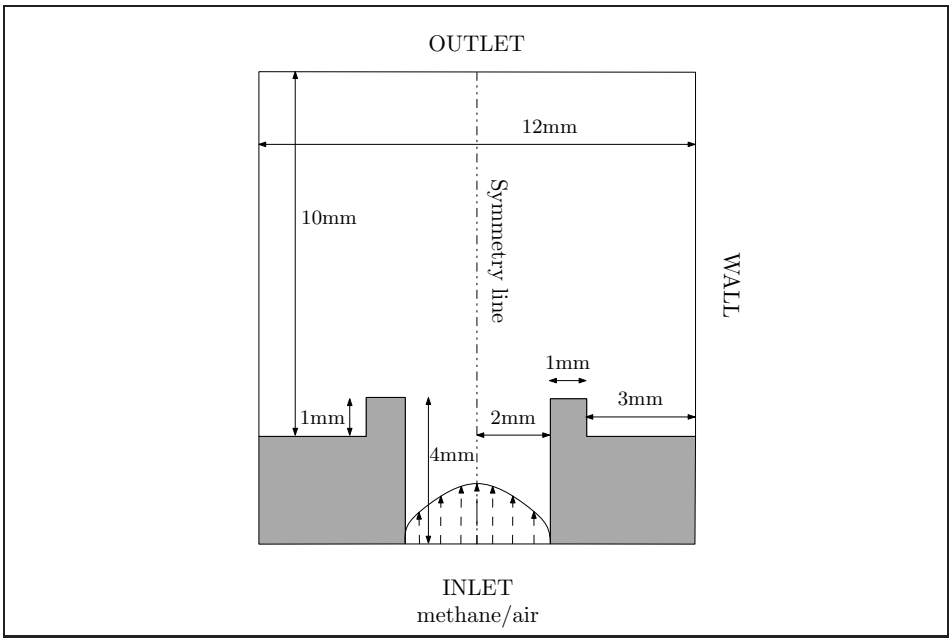

Figure 4.2: Burner configuration (Case 1).

that describe whether flow conditions lead to laminar or turbulent.

$$Re = \frac{UD_H}{\nu} \tag{4.1}$$

where:

- U is characteristic velocity;
- D_H is hydraulic diameter (characteristic length scale);
- ν is kinematic viscosity;

The hydraulic diameter is calculated as:

$$D_H = \frac{4S}{P} = \frac{4ab}{2\,(a+b)} \tag{4.2}$$

where S is the cross-sectional area, B the wetted perimeter, a and b the thickness and the width. For a 2-D geometry $b \to \infty$ thus $D_H = 2a$. While for the characteristic velocity one can take the average which for a laminar parabolic profile is:

$$U_{average} = U_{characteristic} = U_{max} - \frac{1}{3}U_{max} \tag{4.3}$$

	Value	Units of measure
U_{av}	0.733	m/s
D_H	0.004	m
ν	1.5×10^{-5}	m^2/s

Table 4.1: Set of parameters to compute the Re for the case1

with $U_{max} = 1.1[m/s]$.

Using the parameters in the table above, the Reynolds number is to the order of 10^2, which means that the flow field is laminar.

4.2.2 Mesh generation

To create the mesh one has to set up the file `blockMeshDict` in *$caseFolder/constant/polyMesh*, and then typing *blockMesh* command, OpenFOAM reads it and automatically creates mesh and geometry (which are described by the files `points`, `cells`, `faces`, `boundary`). The *blockMeshDict* entries for this case are as follows:

```
/*--------------------------------*- C++ -*----------------------------------*\
| =========                 |                                                 |
| \\      /  F ield         | OpenFOAM: The Open Source CFD Toolbox           |
|  \\    /   O peration     | Version:  1.6                                   |
|   \\  /    A nd           | Web:      http://www.OpenFOAM.org               |
|    \\/     M anipulation  |                                                 |
\*---------------------------------------------------------------------------*/

FoamFile
{
    version     2.0;
    format      ascii;
    class       dictionary;
    object      blockMeshDict;
}
// * * * * * * * * * * * * * * * * * * * * * * * * * * * * * * * * * * * * //

convertToMeters 1e-3;

vertices
(
   (  0    0    0)   //0
   (  4    0    0)   //1
   ( 13    0    0)   //2
   ( 13    2    0)   //3
   ( 13    3    0)   //4
   ( 13    6    0)   //5
```

```
   (  4    6    0)   //6
   (  3    6    0)   //7
   (  3    3    0)   //8
   (  4    3    0)   //9
   (  4    2    0)   //10
   (  0    2    0)   //11
   (  0    0    0.1) //12
   (  4    0    0.1) //13
   ( 13    0    0.1) //14
   ( 13    2    0.1) //15
   ( 13    3    0.1) //16
   ( 13    6    0.1) //17
   (  4    6    0.1) //18
   (  3    6    0.1) //19
   (  3    3    0.1) //20
   (  4    3    0.1) //21
   (  4    2    0.1) //22
   (  0    2    0.1) //23
);

blocks
   (
   hex (0  1  10 11 12  13  22  23)  (20  20  1)  simpleGrading (0.3  1  1) //0
   hex (1  2  3  10 13  14  15  22)  (90  20  1)  simpleGrading (  1  1  1) //1
   hex (10 3  4  9  22  15  16  21)  (90  10  1)  simpleGrading (  1  1  1) //2
   hex (9  4  5  6  21  16  17  18)  (90  20  1)  simpleGrading (  1  2  1) //3
   hex (8  9  6  7  20  21  18  19)  (10  20  1)  simpleGrading (  1  2  1) //4
   );

edges
(
);

patches
(
   patch inletFuel
   (
      (0 12 23 11)
   )

   patch outlet
   (
      (3 15 14 2)
      (4 16 15 3)
      (5 17 16 4)
   )

   wall sideWall
   (
```

```
      (7 19 18 6)
      (6 18 17 5)
      (8 20 19 7)
      (8 9 21 20)
      (10 22 21 9)
      (11 10 22 23)
   )

    symmetryPlane axis
    (
        (0 1 13 12)
        (1 2 14 13)
    )

    empty frontAndBack
    (
        (0 1 10 11)
        (1 2 3 10)
        (10 3 4 9)
        (9 4 5 6)
        (8 9 6 7)
        (12 13 22 23)
        (13 14 15 22)
        (22 15 16 21)
        (21 16 17 18)
        (20 21 18 19)
   )
);

mergePatchPairs
(
);
// ************************************************************************* //
```

To understand better how *vertices*, *blocks*, and *patches* are defined in OpenFOAM check the user guide[11].

4.2.3 boundary and initial condition

In order to solve the problem, both boundary and initial conditions are required for species, pressure, temperature and velocity.

Species

For setting the initial conditions of species, one has to define the condition for N_2, O_2 and CH_4 and $Ydefault$. In $Ydefault$, one has to set the conditions for all

other species not directly defined. The fresh gas mixture methane/air at the inlet is stoichiometric which means that: Y_{N_2} =0.7249, Y_{O_2} =0.22 and Y_{CH_4} =0.0551.

Pressure

The internal field at the time t=0s is supposed to be at the ambient pressure (101325 Pa). Also the outlet, which is at the environment pressure, is set at 1 atm.

Temperature

The burner and chamber walls are maintained at a constant temperature of T_{wall}=298K. The fresh gas temperature is equal to 298 K as well. Normally to ignite the flame it is used to set a high temperature in the internal field; however, in this case this kind of initial condition didn't allow to anchor the flame. Thus, a non-reacting case was launched until it achieved a steady velocity field and species distribution. Then the temperature was increased just in a zone as shown in figure 4.3.It is not advisable to raise the temperature in the entiere geometry because it is fed with the mixture and an explosion would occur, creating instability.

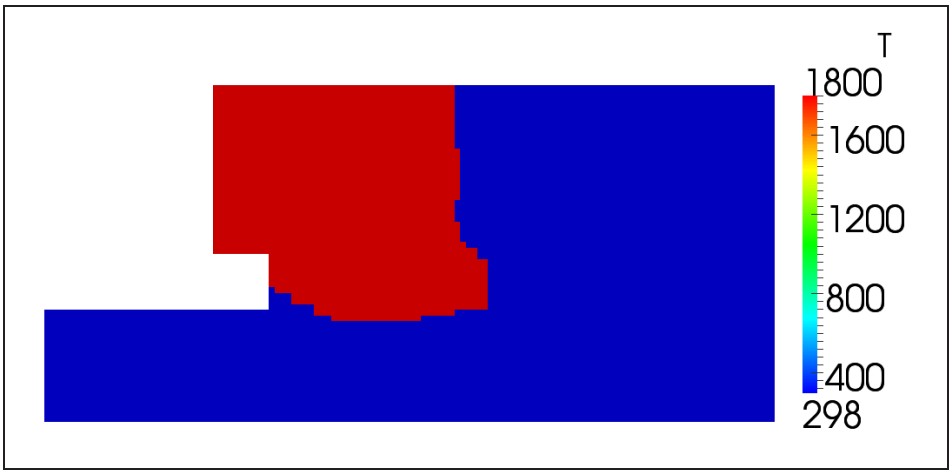

Figure 4.3: T initial condition after species diffusion.

Velocity

The inlet gas velocity profile is parabolic with a maximum value of 1.1 ms^{-1}, while along the walls the velocity is null. In order to create a parabolic profile the *groovyBC* library was used, which allowd one to set non-uniform boundary-conditions without

programming. For further information about this library consult [12].

$$u = u_{max} * \left(1 - \frac{y^2}{Y^2}\right) \tag{4.4}$$

in our case:

- u_{max}= 1.1 ms^{-1};
- Y=0.002 m;

in OpenFOAM it becomes:

```
inletFuel
{
   type groovyBC;
   valueExpression     "vector(1.1*(1-pow((pos().y/0.002),2)),0,0)";
   value                uniform (0 0 0);

}
```

Boundary conditions summary

A summary of all boundary and initial conditions are given in the table below:

	Units	**Inlet**	**Outlet**	**Wall**	**internalField**
N_2	-	0.7249	zeroGradient	zeroGradient	1
O_2	-	0.22	zeroGradient	zeroGradient	0
CH_4	-	0.0551	zeroGradient	zeroGradient	0
Ydefault	-	0	zeroGradient	zeroGradient	0
T	K	298	zeroGradient	298	variable 4.2.3
P	Pa	zeroGradient	101325	zeroGradient	101325
U	ms^{-1}	parabolic	zeroGradient	(0 0 0)	(0 0 0)

Table 4.2: Boundary and initial conditions for the fully premixed case.

Note that the *zeroGrandient* boundary condition at the outlet presumes a flow fully developed.

4.2.4 Reaction mechanism

In the reference paper the chemical scheme used in the computation includes 14 species and 38 reactions, while in our simulation we used the *DRM-19* mechanism, which is a reduced version of *GRI-MECH 1.2* and contains 19 species (+ N_2, AR) and 84 reactions [13]. The *DMR-19* is related in the appendix .3.1.

4.3 Post-processing - case 1

4.3.1 Mesh dependence

The grid independence study has been carried out considering the reacting flow. The refinement is performed with three different meshes and the temperature is kept as the parameter to monitor. Transverse profiles, for different axial positions (y=1 mm, y=3 mm and y=7 mm), of temperature are plotted in figure 4.4 *Mesh A*

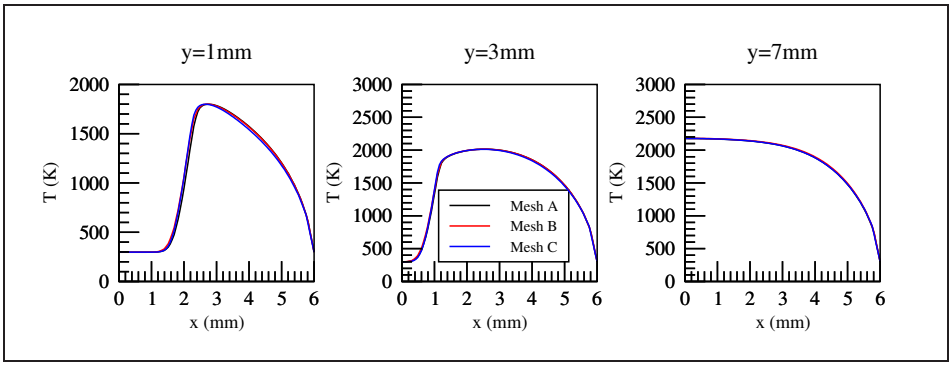

Figure 4.4: Mesh dependence (case-1).

has 5100 cells, *Mesh B* has 4600 and *Mesh C* 10600. The temperature profile for all three meshes is very close to each other especially *Mesh A* and *B* give the some results, and the plot lines are superimposed exactly. In our study the *Mesh A* has been used.

4.3.2 Validation

A comparison between the reference paper and the OpenFOAM results is provided in figure 4.5. On the left-hand side of each figure (called A) is plotted the reference solution by [2], while the OpenFOAM results are presented on the right-hand side (called B). This comparison shows that the main features of the flame such as the flame-front position and maximum level of temperature are pretty well reproduced (the relative error of maximum level of temperature is smaller than 5%). Minor species such as HCO are also well estimated and localized.

To check more efficiently the difference between the two solutions (fig.4.6), we present crosssectional profiles of CO_2, H_2O and CO obtained at 1 mm, 3 mm, and 7 mm above the burner lips. These profiles show good agreement even for minor species like CO. The OpenFOAM result is slightly shifted to the right compared to the reference case. These error in the temperature prediction can be attributed to the fact that two different chemichal mechanisms have been used.

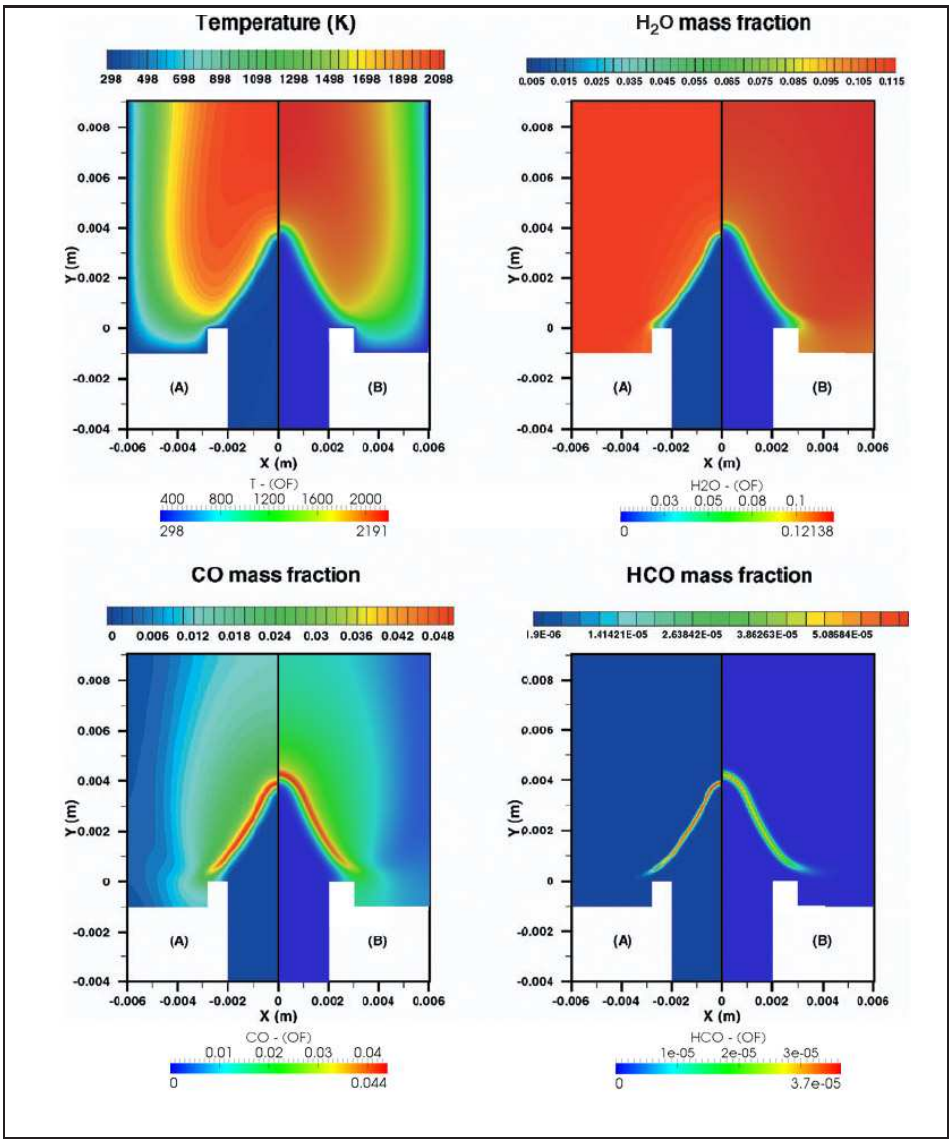

Figure 4.5: Mesh dependence (case-1).

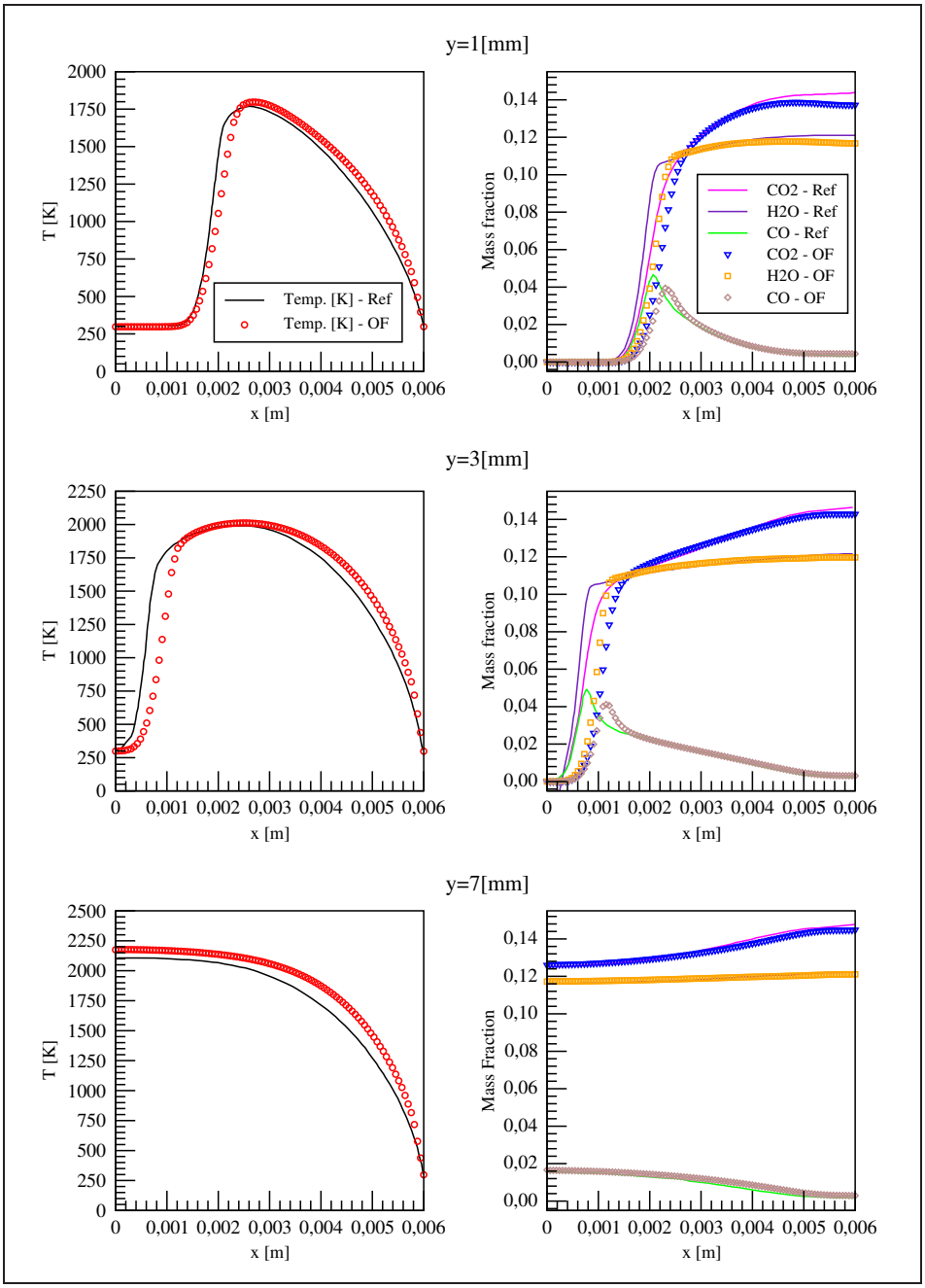

Figure 4.6: Profiles of temperature and mass fractions of H_2O, CO_2 and CO.

4.4 Preprocessing - case 2

The second burner configuration is shown in figure 4.7 . Methane is mixed with air and injected through the central slot before entering into the combustion chamber. Then there are two secondary inlets besides the primary one where there is air incoming. The computation has been done for half of the domain because of the symmetry geometry of the burner.

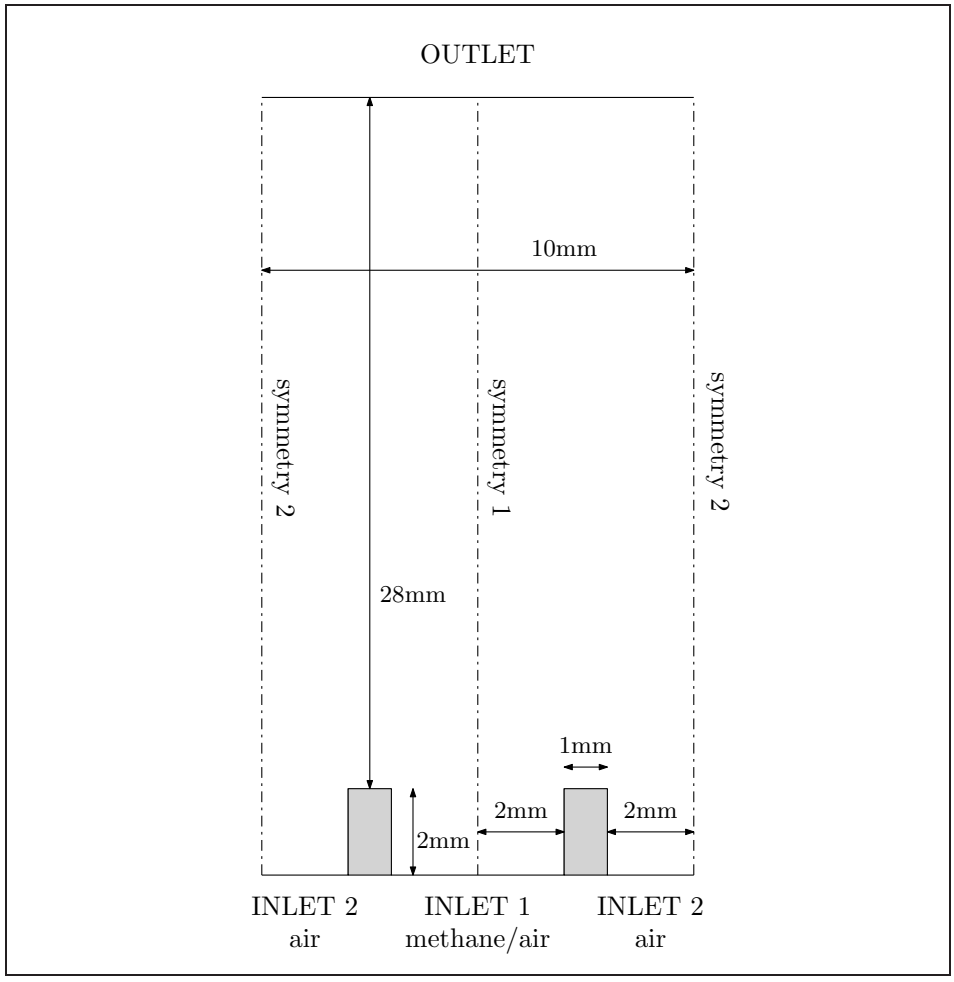

Figure 4.7: burner configuration (Case 2).

4.4.1 Regime flow

The primary and secondary inlet have a velocity constant and equal to 1.0 ms^{-1} and 0.05 ms^{-1} and the width of the slots are 4 mm and 2 mm respectively. In order to

calculate the Reynolds number we used the primary inlets and it is to the order of 10^2 which mean that the flow is laminar.

4.4.2 boundary and initial condition

The boundary and initial conditions are resumed in the table below.

	Units	**prim.Inlet**	**sec.Inlet**	**int.Field**	**Injector Wall**	**Outlet**
N_2	-	0.7253	0.7653	1	zeroGradient	zeroGradient
O_2	-	0.2224	0.2347	0	zeroGradient	zeroGradient
CH_4	-	0.0523	0	0	zeroGradient	zeroGradient
Ydefault	-	0	0	0	zeroGradient	zeroGradient
T	K	298	298	1900	298	zeroGradient
P	Pa	zeroGradient		101325	zeroGradient	101325
U	ms^{-1}	1	0.05	(0 0 0)	(0 0 0)	zeroGradient

Table 4.3: Boundary and initial conditions used for the partially premixed case.

4.4.3 Reaction mechanism

In the reference paper for this computation, the detailed mechanism of Lindstedt has been employed (29 species and 300 reactions), while in OpenFOAM model the DRM-19 .3.1 mechanism has been used.

4.5 Post-processing - case 2

4.5.1 Mesh dependence

Also for this case, as well as for the fully premixed one, the grid independence study has been carried out considering the reacting flow. The refinement is performed with three different meshes and the temperature is kept as parameter to monitor. Transverse profiles, for different axial positions (y=2 mm, y=5 mm and y=8 mm), of temperature are plotted in figure 4.8 *Mesh A* has 3410 cells, *Mesh B* 7650 and, *Mesh C* 11050. The temperature profiles for *Mesh B* and *Mesh C* are very close. In our study the finer mesh has been chosen.

4.5.2 Validation

Colored isolevels of temperature, CO, H_2O and HCO mass fractions are plotted in figure 4.9 for both reference (left, A) and the computations with OpenFOAM (right, B). As for the fully premixed flame, the OpenFOAM results are in good agreement

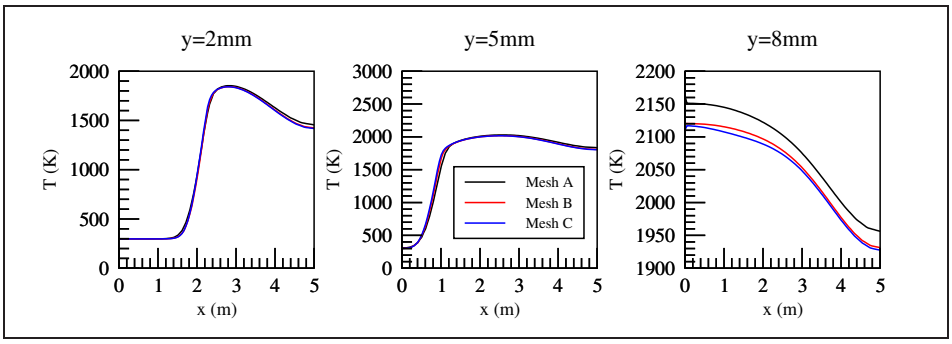

Figure 4.8: Mesh dependence (case-2).

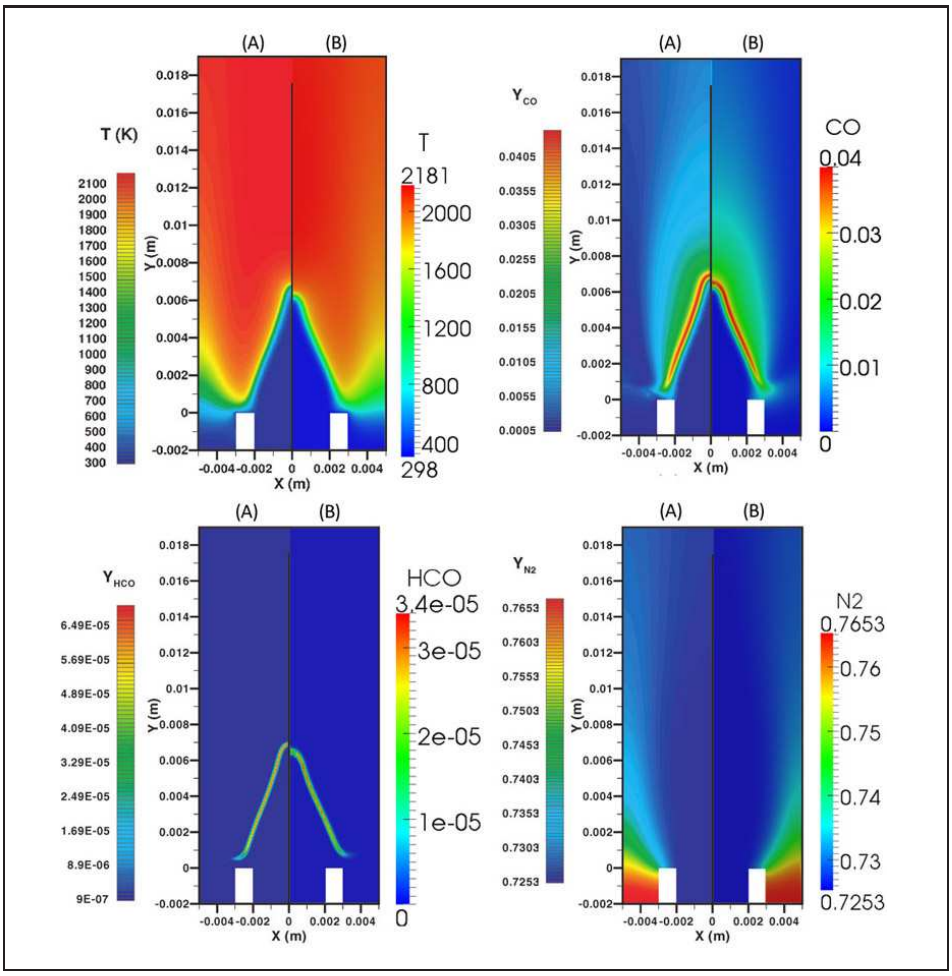

Figure 4.9: Qualitative comparison between OpenFOAM and reference results

with reference. Transverse profiles, for different axial positions (y=2 mm, y=5 mm and y=8 mm), of temperature, CO_2 , H_2O and CO mass fractions are plotted in figures 4.10

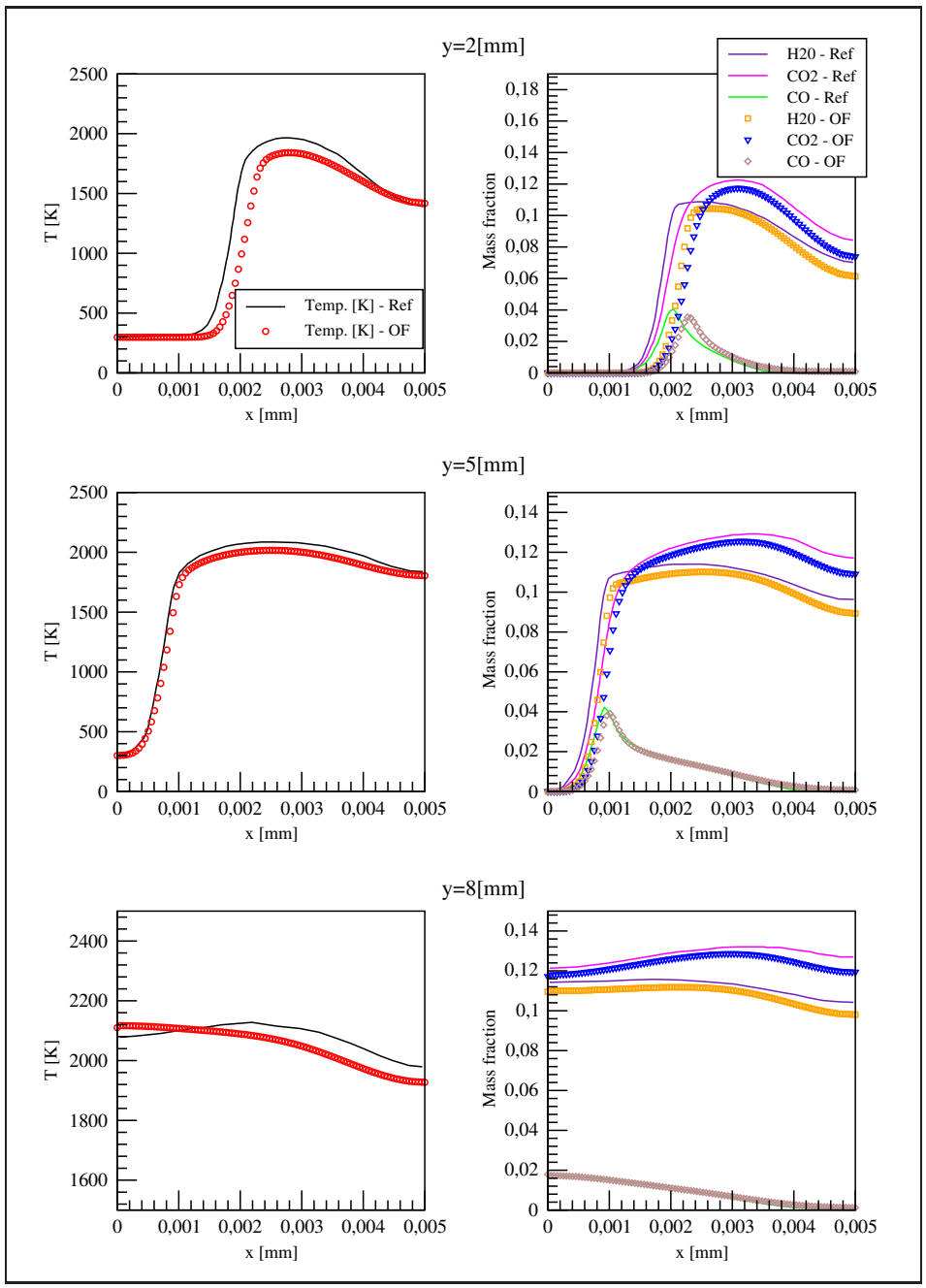

Figure 4.10: Profiles of temperature and mass fractions of H_2O, CO_2 and CO.

For the plot at the axial position y=8 mm there is a slight diasagreement between the two temperature trends. This is due to the difference of flame height in the reference model and the one obtained with OpenFOAM. Indeed also if it is a small difference in this zone, just on top of the flame, there is a huge temperature gradient, and resulting in big differences of temperature along the axial direction. Taking into account the flame height difference and plotting the temperature along the transversal profile at an axial position of y=7.3 mm instead of 8 mm (figure 4.11) there is a more remarkable agreement with the reference temperature profile.

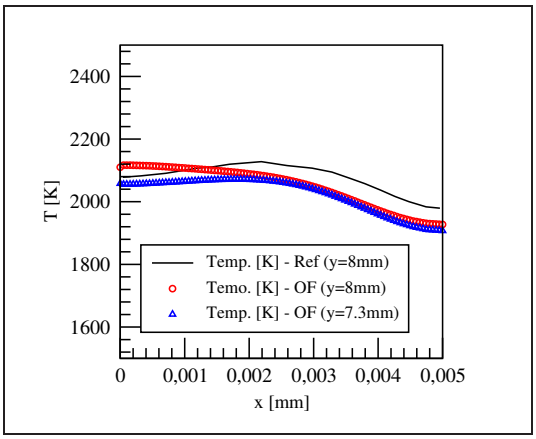

Figure 4.11: Transverse profile of temperature at y=7.3mm and y=8mm (case-2).

4.6 Conclusion

The comparisons between the reference and OpenFOAM results is quite accurate even though some discrepancies are present. These disagreements can be attributed to two causes:

- mesh
- chemical mechanism.

Indeed in the reference model, an adapted mesh was used. It allows to have a very fine grid in correspondence to the flame front, where big gradients are present. However, the mesh used in this work was fine enough to have good temperature prediction, and also the minor species like HCO and CO are well reproduced. In the chemical mechanism are defined all the reactions and their coefficients. Using two different mechanisms can lead having different heat release, which means a different temperature and thus, different species concentrations as well. However, these results are satisfactory and a turbulent model will be developed.

Chapter 5

Turbulent Case

5.1 Introduction

In this section we will study an axisymmetric dump combustor. In the dump combustors flow expands over a step producing a strong recirculation zone that helps in flame stabilization. Experimental data[15] are available for this combustor and Fluent studies [16] have already been done which give the opportunity to compare them with the OpenFOAM ones.

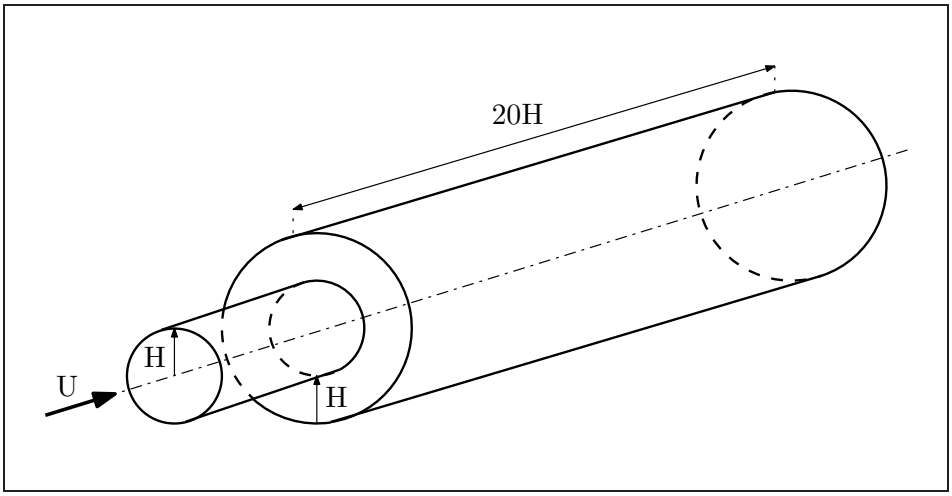

Figure 5.1: Schematic of the axissymmetric dump combustor

The schematic of the combustor geometry is shown in figure 5.1. The combustor has a step height of H= 38.1 mm and the inlet radius equal to H. The radius of combustor is $2H$ and its length is $20H$. The domain is axisymmetric thus the model is reduced to a 2-D case. The Computational domain is shown in figure 5.2

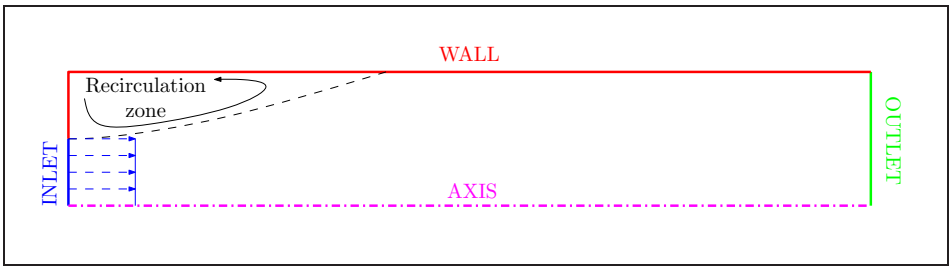

Figure 5.2: Computational domain (axissymmetric dump combustor)

5.2 Pre-processing

5.2.1 Flow regime

The inlet velocity is U=22 ms^{-1} and the incoming gas is a mixture of propane/air. The inlet radius is of 38.1 mm. The set of parameters to compute the Reynolds number are shown in table below:

	Value	**Units of measure**
U_{av}	22	m/s
D_H	0.0381	m
ν	1.59×10^{-5}	m^2/s

Table 5.1: Set of parameters to compute the Re

Using equation (4.1) the Reynolds number for this flow is of the order of 10^4 and this means that the flow is totally turbulent.

5.2.2 Boundary and initial conditions

Species

The inlet flow is a completely premixed propane/air mixture. The equivalence ratio is $\Phi = 0.5$. Air is assumed to be a mixture of N_2 and O_2. Thus the inlet species mass fractions are:

- $Y_{O_2} = 0.203466$;
- $Y_{N_2} = 0.76542255$;
- $Y_{C_3H_8} = 0.03111145$.

Pressure

The internal field is assumed to be at atmospheric pressure (101325 Pa) and the outlet as well. The reactingFoam solver takes into account the compressibility of the gas, which means the pressure waves, that are reflected from the outlet, give instability in the flow if a not appropriate boundary condition is chosen. Thus in the model *waveTransmissive* boundary condition is used to allow pressure waves to exit the domain without reflections.

```
outlet
    {
       type            waveTransmissive;
       value           uniform 101325;
       gamma           1.4;
       field           p;
       lInf            0.5;
       fieldInf        101325;
    }
```

where:

- `value` is important to correct I/O
- `gamma` is the ratio of specific heats
- `field` is the name of the field that we are working on
- `lInf` is a measure of how far away the far-field condition should be (in meters)
- `fieldInf` the far-field value to be applied to p

The larger the value of `lInf`, the further the boundary condition will deviate from the value specified as `fieldInf`. However, the smaller the value of `lInf`, the more reflective the boundary tends to be [17].

Temperature

The incoming cold flow is at 298 K. In the experimental work [15] the temperature boundary conditions at the wall were not specified. In the Fluent work [16], it was assumed 298 K, thus in this work the same condition has been set up. The temperature field initial condition is set to 2000K to imitate the ignition process.

Velocity and Turbulence

The mixture of propane/air enters in the combustor at a constant and flat velocity velocity profile of $U = 22$ ms^{-1} and with a turbulent intensity $I = 5\%$. Inlet value for kinetic energy k is computed using the following eqution:

$$k = 1.5\,(U_{av} * I)^2 = 1.815(m^2/s^2) \tag{5.1}$$

where U_{av} is the average of velocity (for the instance 22 ms^{-1}). The value of ϵ at the inlet can be estimate as:

$$\epsilon = \frac{C_\mu^{3/4} k^{3/2}}{l} = 150.65(m^2/s^2) \tag{5.2}$$

where the constant $C_\mu = 0.09$,the turbulent length scale $l = 0.07 D_H$ (D_H is the Hydraulic diameter). In OpenFOAM there are some specific boundary conditions for the wall to handle the k-ϵ model called *WallFunction*. The inlet and wall boundary conditions for k in the input file read

```
inletFuel
    {

        type            turbulentIntensityKineticEnergyInlet;
        intensity       0.05;
        value           uniform 1.815;
    }
sideWall
    {
        type            compressible::kqRWallFunction;
        value           uniform 1.815;
    }
```

and for ϵ

```
inletFuel
    {
        type            fixedValue;
        value           uniform 150.65;
    }
sideWall
    {
        type            compressible::epsilonWallFunction;
        Cmu             0.09;
        kappa           0.41;
        E               9.8;
        value           uniform 150.65;
    }
```

The outlet boundary conditions are *zeroGradient* for k, ϵ and velocity.

Boundary conditions summary

A summary of all boundary and initials conditions are given in the table below

	Units	Inlet	Outlet	Wall	internalField
N_2	-	0.76542255	zeroGradient	zeroGradient	1
O_2	-	0.203466	zeroGradient	zeroGradient	0
C_3H_8	-	0.03111145	zeroGradient	zeroGradient	0
T	K	298	zeroGradient	298	2000
P	Pa	zeroGradient	waveTransmissive	zeroGradient	101325
U	ms^{-1}	22	zeroGradient	(0 0 0)	(0 0 0)
k	m^2s^{-2}	1.815	zeroGradient	wallFunction	1.815
ϵ	m^2s^{-2}	150.65	zeroGradient	wallFunction	150.65

Table 5.2: Boundary and initial conditions (dump combustor).

5.2.3 Reaction mechanism

A single-step reaction has been used in this work. The mechanism is showed below

```
ELEMENTS
H   O    C   N
END

SPECIE
O2  H2O  CO2  N2  C3H8
END

REACTIONS
C3H8 + 5O2 => 3CO2 + 4H2O         8.6e11     0    30000
FORD / C3H8 0.1 /
FORD / O2  1.65 /
END
```

5.2.4 Turbulent model setup

As discussed in the previous chapter the chemistry and turbulence properties are set in files present in $\$case/constant$ folder. The most important ones are:

- `turbulenceProperties` where the type of simulation is chosen (RANS or LES).

```
//*********************************************************************//

simulationType  RASModel;

//*********************************************************************//
```

- `RASProperties` within the turbulence model is set up (k-epsilon, k-omega...) and also the relative coefficients. If the coefficients are not declared in this file OpenFOAM uses the default ones.

```
//*********************************************************************//

RASModel        kEpsilon;

turbulence      on;

printCoeffs     on;

kEpsilonCoeffs
    {
        Cmu         0.09;
        C1          1.44;
        C2          1.92;
        C3          -0.33;  // only for compressible
        sigmak      1.0;    // only for compressible
        sigmaEps    1.3;
        Prt         0.95;    // only for compressible
    }

//*********************************************************************//
```

- `chemistryProperties` where the ODE solver is chosen and the constant Cmix is set up.

```
//*********************************************************************//

psiChemistryModel  ODEChemistryModel<gasThermoPhysics>;

chemistry           on;

chemistrySolver     ode;

initialChemicalTimeStep 1e-08;

turbulentReaction   on;

sequentialCoeffs
{
    cTauChem        0.001;
}

EulerImplicitCoeffs
{
    cTauChem        0.05;
    equilibriumRateLimiter off;
```

```
}

odeCoeffs
{
    ODESolver       SIBS;
    eps             0.05;
    scale           1;
}

Cmix            Cmix [ 0 0 0 0 0 0 0 ] 15;

//************************************************************************//
```

- `thermophysicalProperties` where the chemichal mechanism and the species thermo-data are set up. The inert species are also declared here.

```
//************************************************************************//

thermoType hsPsiMixtureThermo<reactingMixture<gasThermoPhysics>>

inertSpecie N2;

chemistryReader chemkinReader;

CHEMKINFile                 "$FOAM_CASE/constant/oneStepC3H8";
CHEMKINThermoFile           "$FOAM_CASE/constant/therm.dat";

//************************************************************************//
```

  where `oneStepC3H8` is the name of the file containing the reaction mechanism (in this instance the one-step reaction for propane) and `therm.dat` is the thermo-data file.

5.3 Post-processing

5.3.1 Mesh study

In this work, the grid independence study has been carried out considering the reacting case. Strictly speaking, a mesh independent study should be done also for the cold flow case. However, it is reasonable to assume that the grid for which mesh independence has been proved in the case of reacting flow may also be used in the cold flow case.

The mesh-refinement study was performed with three levels of refinement.

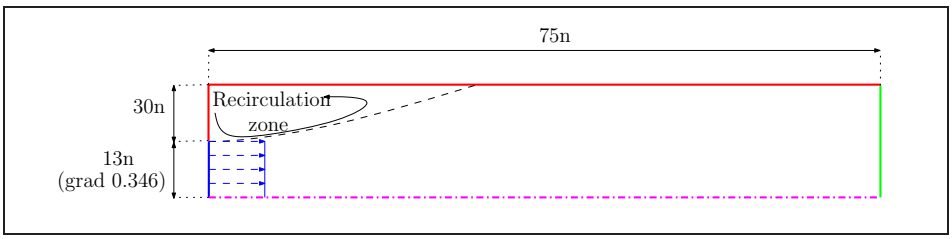

Figure 5.3: Mesh distribution (hexahedral cells)

- Initail mesh: n=2 - *Mesh A* - 12750 cells;
- First refinement: n=2.5 - *Mesh B* - 20116 cells;
- Second refinement: n=3 - *Mesh C* - 35200 cells.

As we told in the introduction section this dump combustor geometry has been already studied in the past with Fluen[16]. In that case the mesh distribution is described by figure 5.3 imposing n=2. Therfore starting for that mesh two refinements have been done.

In figure 5.4, the normalized axial velocity comparison for three meshes is shown. Where U_{ref}= 22 ms^{-1} is the reference velocity. There is a good agreement between the cases, except for the results at section x/H=12 where a small discrepancy is present between the finer mesh and the other two. It is due to the lower temperature for *Mesh C* which means a smaller expansion and velocity as well.

Figure 5.5 shows the plots for normalize temperature (T_{ref} = 298 K). Form these plots one can see that a mesh convergence for temperature is not present. Actually on the flame front there are large gradients and to predict them correctly a very fine mesh is necessary. The best way to do this is use the *local mesh refinement* which provides a fine mesh where large gradients are presents; in this work such mesh has not been used. Even though the temperature plots would suggest a further

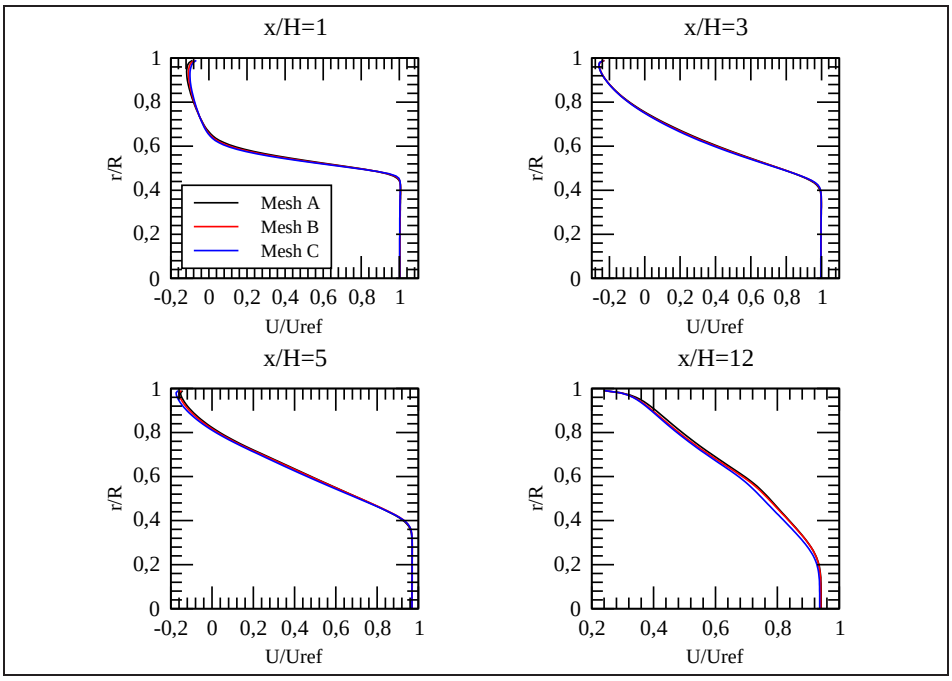

Figure 5.4: Normalized axial velocity - mesh study

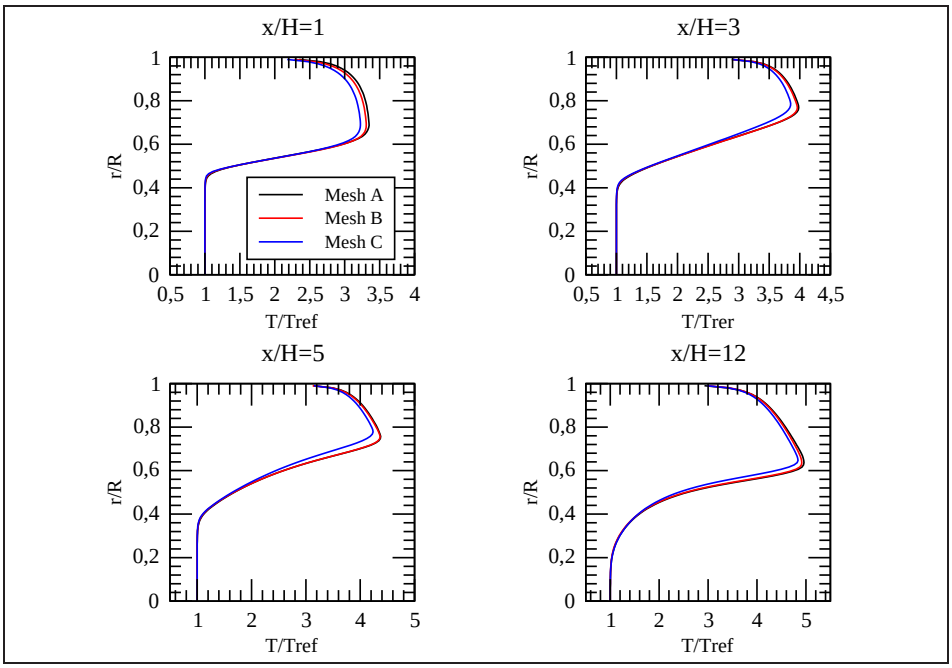

Figure 5.5: Normalized temperature - mesh study

refinement of the mesh the flow field is already stable and the *Mesh A* was used to study the case which is shown in figure 5.6

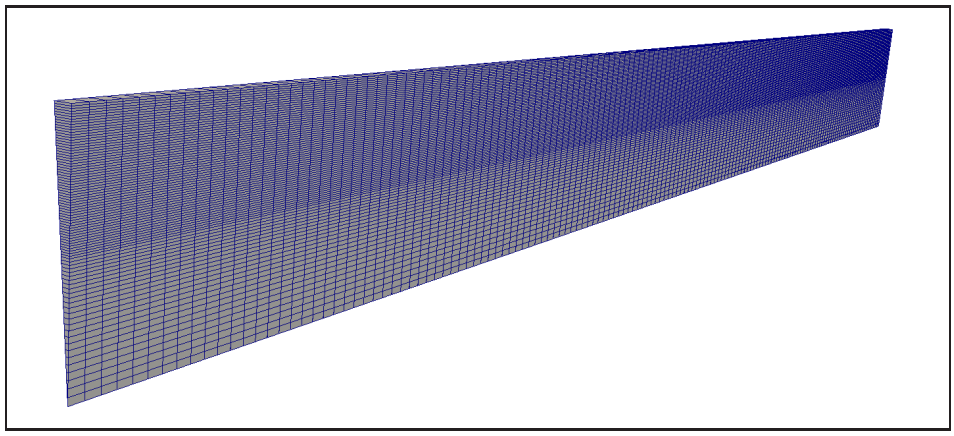

Figure 5.6: mesh used (axisymmetric dump combustor)

Temperature field and the streamlines for velocity for *Mesh A* are shown in figure 5.7. It is improtant to notice the effect of recirculation zone which anchors the flame. The front flame speed for propane is about 0.4 ms^{-}1 that is two order of magnitude smaller than the axial velocity field. Thus, high temperature products are captured in the recirculation zone, and this in turn ignites the incoming cold reacting species.

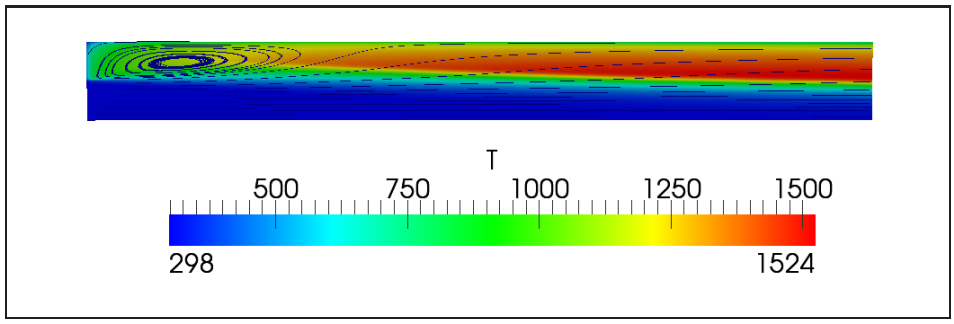

Figure 5.7: Temperature field [K] and velocity streamlines

5.3.2 Cold flow

To make sure that all the turbulent and fluid boundary conditions were well setted up and to convalidate the k-ϵ model a cold flow analysis have been done. A comparison of OpenFOAM results for turbulent kinetic energy k, radial velocity V and axial

velocity U with Fluent ones and experimental data are reported in figure 5.8, 5.9 and 5.10 respectively.

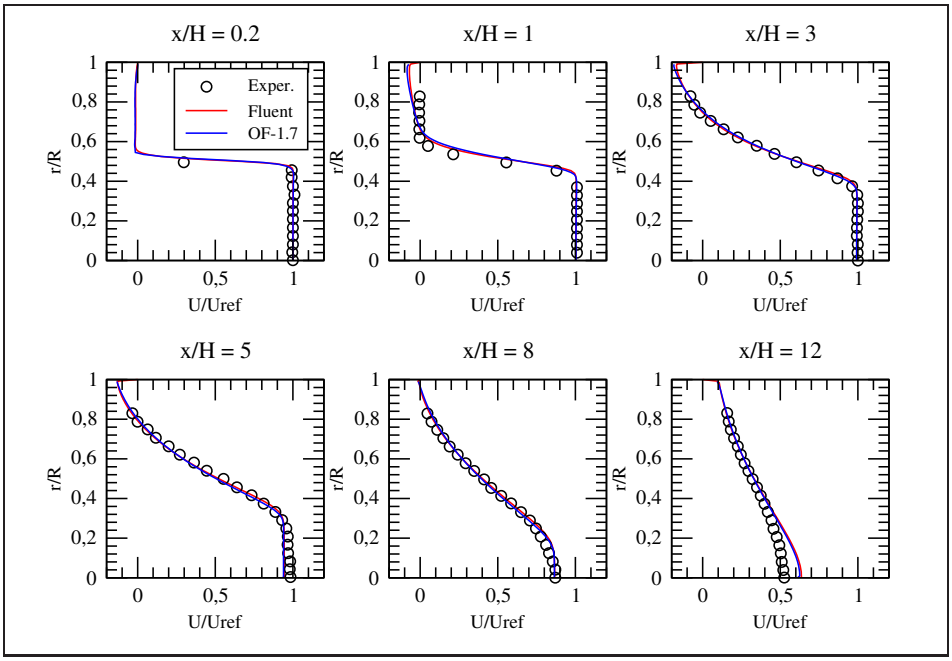

Figure 5.8: Normalized axial velocity (U) of cold flow

The figure 5.8 shows a good agreement between the experimental data and the predictions with both Fluent and OpenFOAM. Also, for the radial velocity the values predicted by OpenFOAM and Fluent are close to each other but some differences when compared to experimental data (figure 5.9). The source of this discrepancy is not obvious, but the present results are internally consistent and exhibit no anomalies. The predicted mean radial velocities agree qualitatively with the measured and values are within the uncertainty estimate over most of the flow. Differences between predicted and measured values are largest in the recirculation zone.

Figure 5.10 shows the normalized turbulent kinetic energy profiles. The agreement between the computed and measured values is quite good for $r/R < 0.8$ then some discrepancies are present. One must remember that the k-ϵ model does not directly predict turbulent stresses; it solves two additional conservation equations , one for turbulent kinetic energy and one for turbulent dissipation rate, in order to define an eddy viscosity. Furtheremore, it solve mean value of the quantities. Thus, the presence of some discrepancies between experimental data and numerical results are acceptable and the predictions of the turbulent quantities in the dump combustor are good.

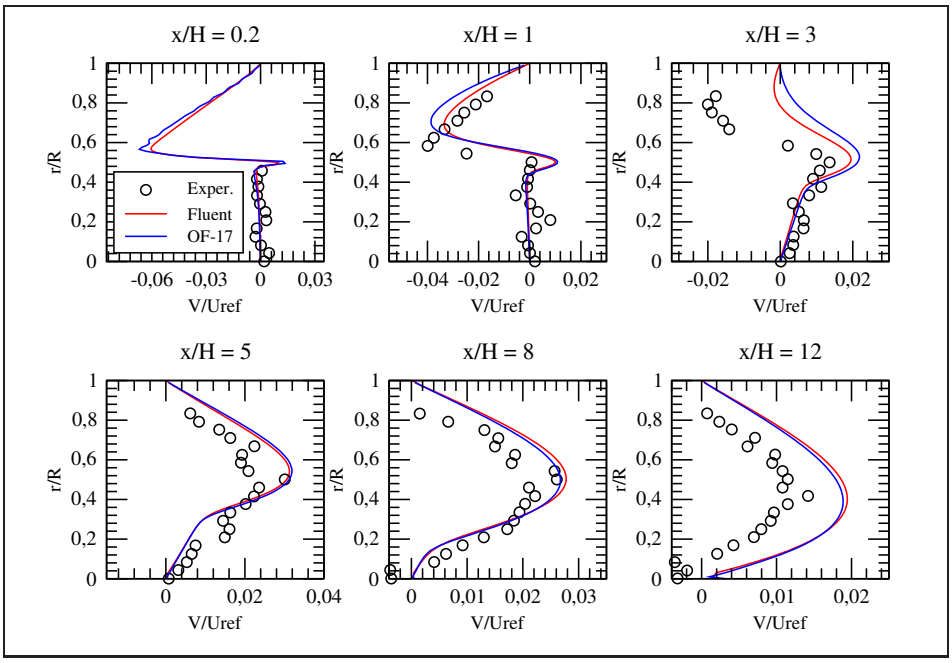

Figure 5.9: Normalized radial velocity (v) of cold flow

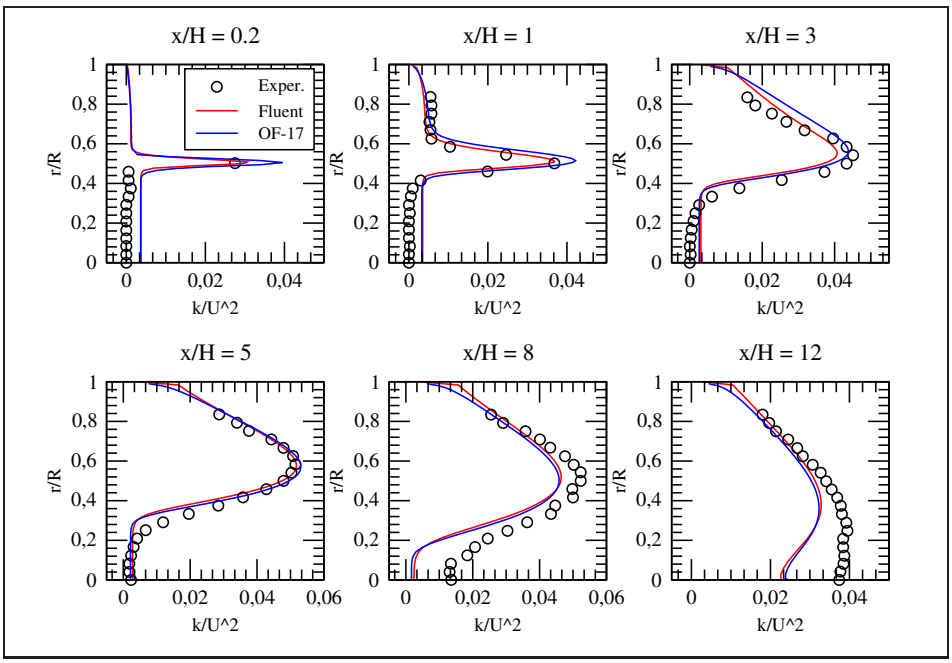

Figure 5.10: Normalized turbulent kinetic energy (k) of cold flow

5.3.3 Probes

The solver reactingFoam used for the simulations is a transient one, and it must be run until the steady state is achieved. In order to understand when the steady state has been reached the time evolution of temperature, axial and radial velocity have been monitored at four points in the domain 5.11. The locations of the probes are specified in the file `probeDict` which is in the `system` directory.

	Axial direction x/H	**Radial direction** r/R
Probe 1	1	1/2
Probe 2	3	1/2
Probe 3	5	1/2
Probe 4–	12	1/2

Table 5.3: Probes' positions

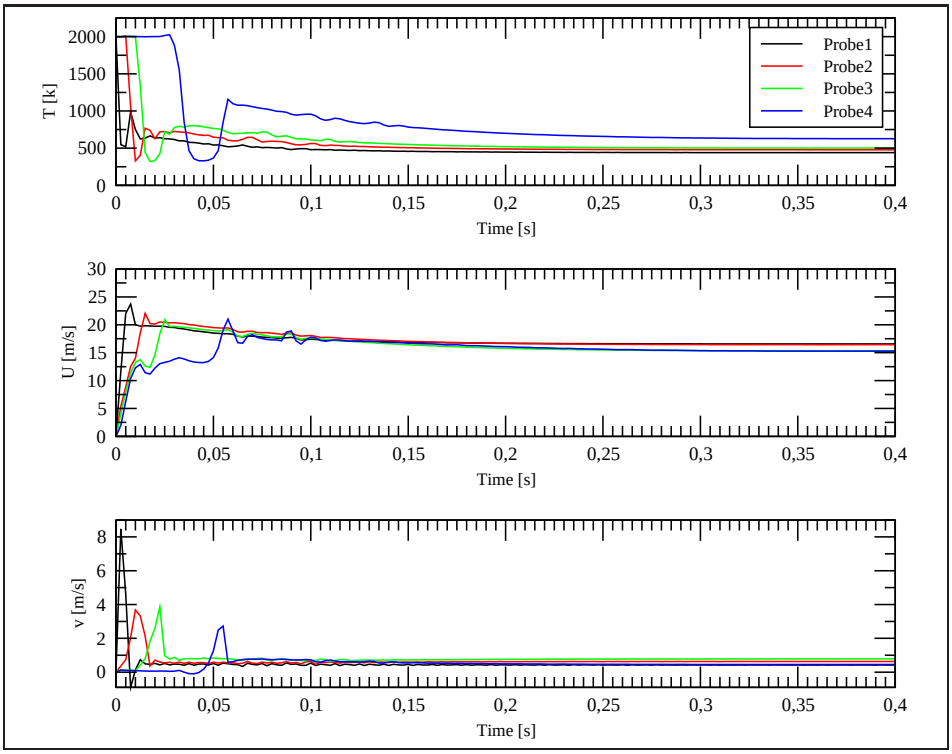

Figure 5.11: Probes for Temperature axial and radial velocity

Figure 5.11 shows that a trasient occurs at the beginning of the simulation than at about 0.35s the flows reachs the stady state.

5.3.4 Influence of *Cmix*

As described in the section 3.2.3 the combustion model used in this work is the *Chalmers PaSR-Model* which presumes to calculate the reactive fraction κ by the formula 3.6 that is quickly reminded here below

$$\kappa = \frac{\tau_f + \tau_c}{\tau_f + \tau_c + \tau_{mix}}$$

The only term in this equation that one can directly play with is τ_{mix}. Modifying the value of the constant *Cmix*: higher is *Cmix* bigger is the τ_{mix} and in turn the effects of the mixing in the model. A parametrization study of *Cmix* is shown in figures 5.12 and 5.13 with temperature and axial velocity profiles respectively. These results are compared with the Fluent results and experimental data. For a small

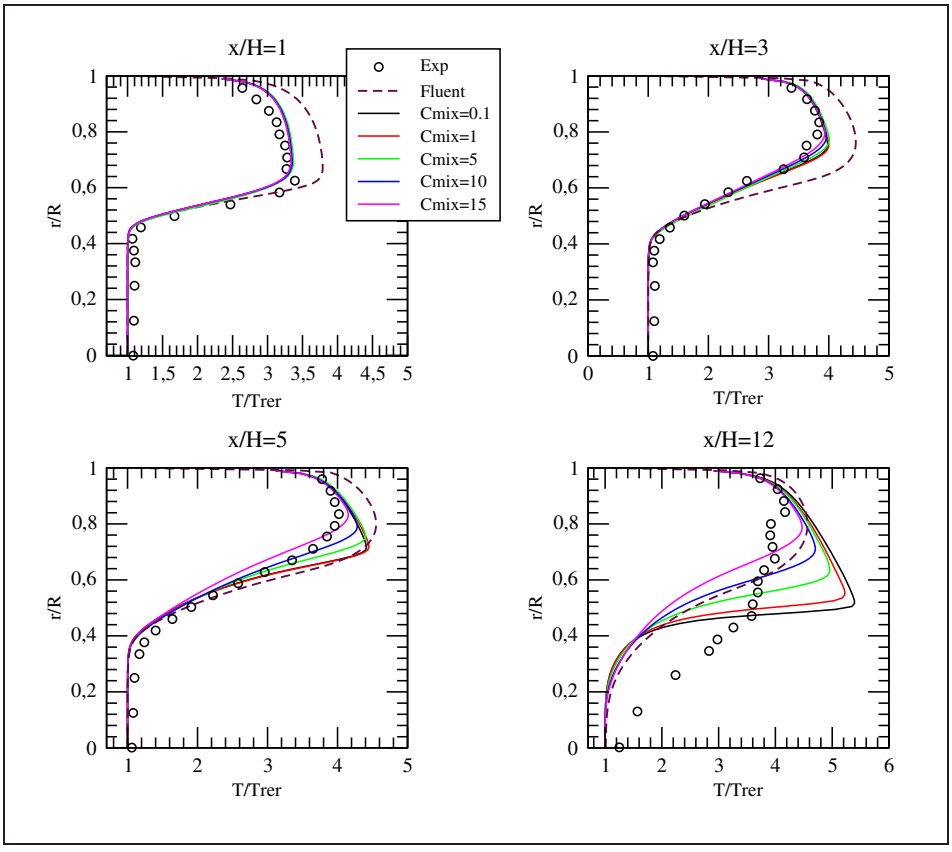

Figure 5.12: Normalized Temperature for different Cmix

value of *Cmix*, the trend of temperature is very sharp. Basically it means that the reactions are much faster than the mixing rate. Therefore, the heat is released in a very thin area causing the temperature to rise lot close to the flame front leading

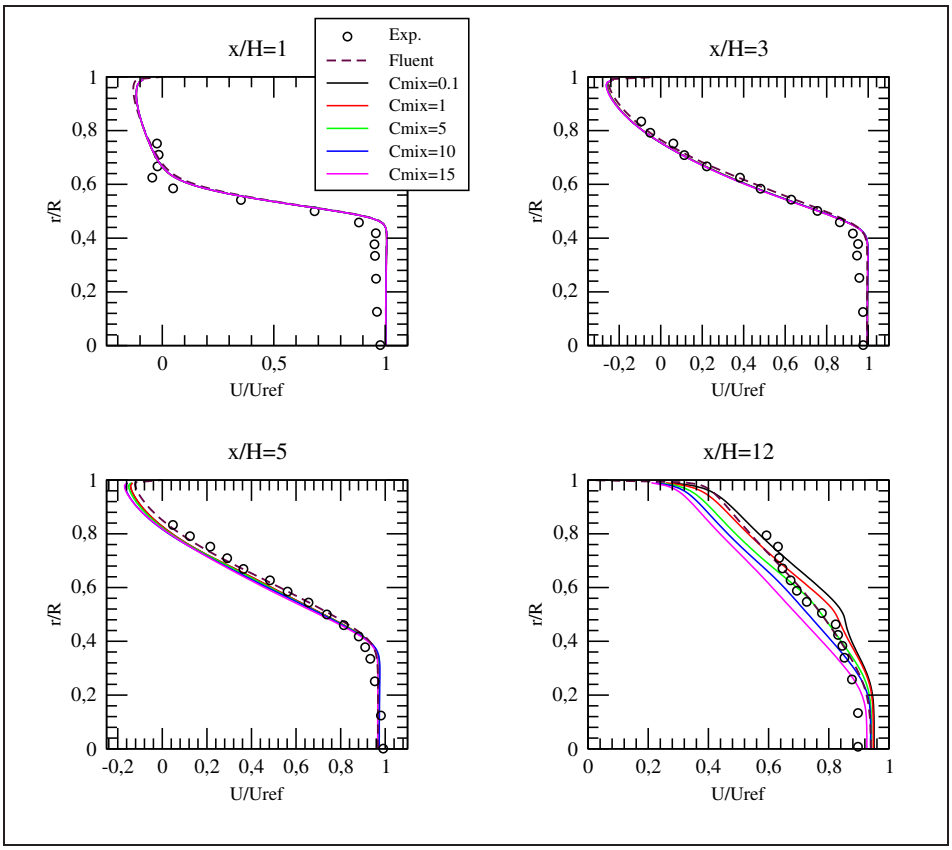

Figure 5.13: Normalized axial velocity for different Cmix

to phenomenon called laminarization of the flow. Essentially the turbulence effect drop down in this area and as a consequence the effect of turbulent viscosity and turbulent thermal diffusivity are reduced.

Whereas, $Cmix$ does non have big influence on the vecolity field except for the profiles at the axial position x/H=12, which is the one where the lamanarization effet is more present. In this chart is possible remarke that axial velocity decreses and its profile becomes smoother with big $Cmix$. This is due to the fact that the laminarization effect decrease end μ_t rise.

In figure 5.14 it is possible to notice how the turbulet viscosity field and the heat release change for different values of $Cmix$. One must remember that in this work the turbulet Prandtl number has been kept constant (Pr=0.95). Hence, the shapes of turbulent viscosity and turbulent thermal diffusivity are the same. It is remarkable that larger $Cmix$ values reduce the laminarization effect and thus a smoother profile for temperature is obtained.

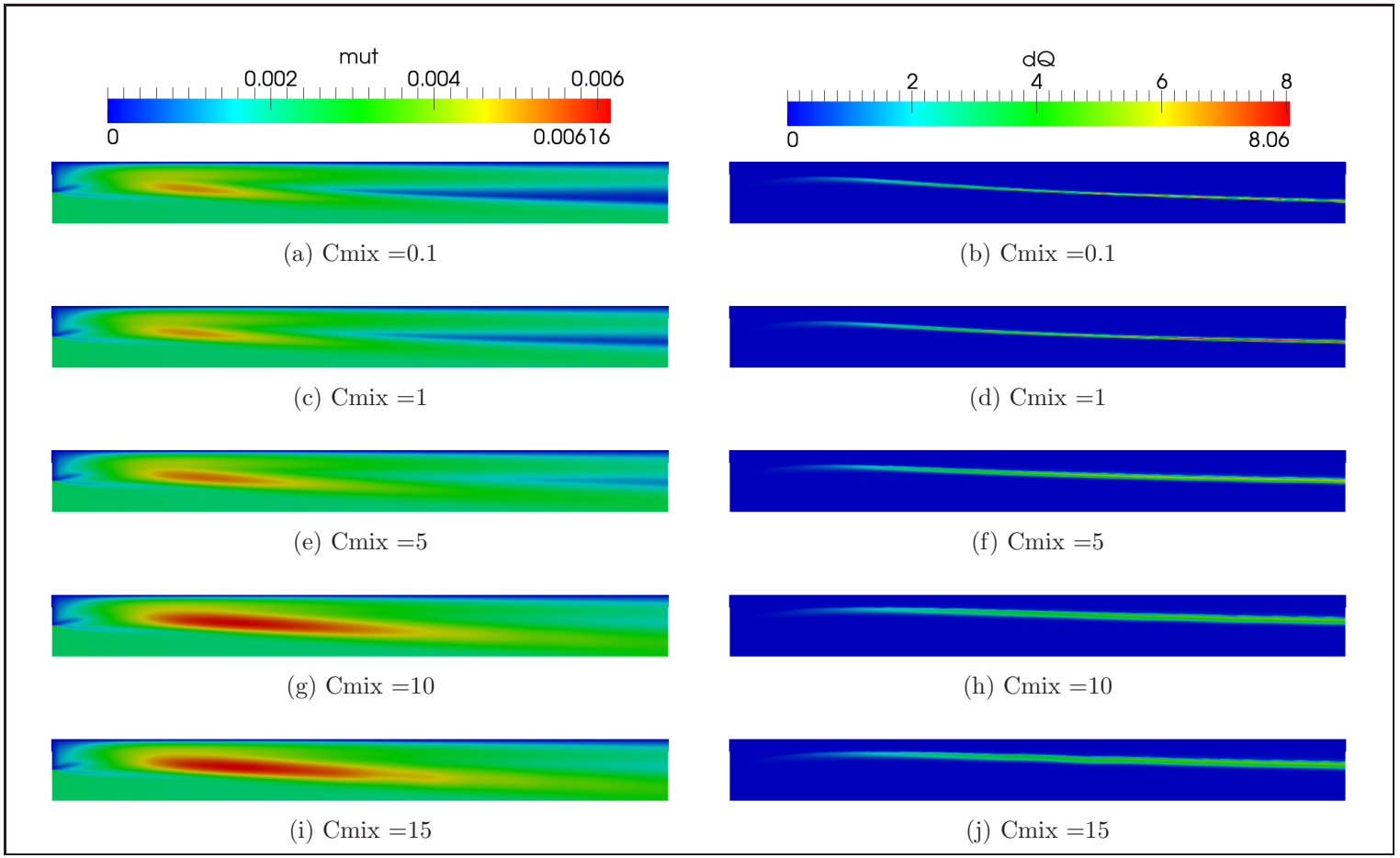

(a) Cmix =0.1 (b) Cmix =0.1

(c) Cmix =1 (d) Cmix =1

(e) Cmix =5 (f) Cmix =5

(g) Cmix =10 (h) Cmix =10

(i) Cmix =15 (j) Cmix =15

Figure 5.14: turbulet viscosity (left) and heat relaese (right) for differnt Cmix

5.4 Conclusion

The prediction for a cold flow is good even though some discrepancies with the experimental data are present. Though they are reasonably acceptable considering the fact that the turbulent kinetic energie and turbulent dissipation are predicted using the $k - \epsilon$ model which is a Reynolds-averaged Navier-Stokes (RANS) model.

Some disagreement are present for the temperature prediction between the fluent and OpenFOAM results. Infect the Fluent solution does not present any laminarization effects, which, on the other hand, occurs using OpenFOAM. The source of this difference is probably the turbulent combustion model. Indeed, OpenFOAM uses the *PaSR* model, while in fulent the *Eddy Break Up* model is employed. The disavantage of using the eddy brack up model is that only a single-step reaction mechanism can be employed. Forthermore for axial positions closer to the inlet, where the laminarization is not yet presents, the temperature predicion is more accurate with OpenFOAM.

.1 alternateReactingFoam test cases

As we discussed in the introduction we decided to stop using alternateReactingFoam solver because the version 1.5 of OpenFOAM presented some problems when handling the mixing process. Figure 15 shows an adiabatic square geometry filled by two columns of two different species (propane and nitrogen) and they were left to mix. Only the mixing process is studied, which means there are no reactions present. The initial temperature is 298 K.

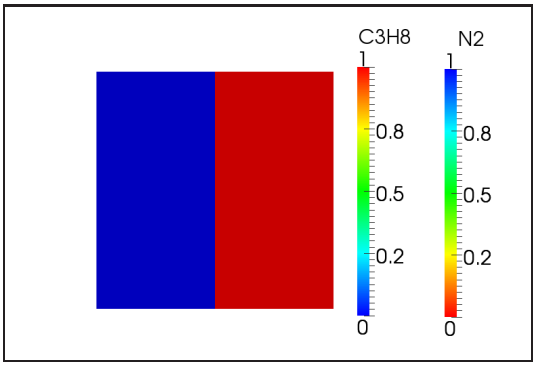

Figure 15: Initial species distribution (blue=N_2, red=C_3H_8).

Figure 16 shows the temperature field for different time steps. The temperature field is presumed to be constant for a non-reactant flow, but for some reason it is not. Furtheremore, when the steady state is reached, its value is different from the initial one. It is an adiabatic non-reacting case which mean that the temperature field behavior is notably wrong.

This problem occurs also in a premixed flame. Indeed, in combustion some species are created and they are mixed with the ones already present. Figure 17 shows the temperature field for the fully premixed case studied in the section 4.2. The temperature range was rescaled imposing a maximum of 500 K in order to show the low temperature zone more clearly. The steady solution of reactingFoam (OF-1.7) was used as initial condition.

The first time step is the solution with reactinFoam (OF-1.7). In the following ones it remarkable that just under the flame front, a low temperature zone is occurs, which makes the flame unstable.

The same results are obtained with reactingFoam (OF-1.5). As show in the section 2.3.2, OpenFOAM 1.5 solves a total enthalpy equation with the assumption of unity Lewis number (Le=1). If instead of Le=1 a unity Schmidt number is assumed, the temperature does not drop anymore during the mixing process. Though, in alternateReactinFoam this change is not at all trivial because one needs to have access to the enthalpy h_i of the different species, but the alternateSolver only needs, and

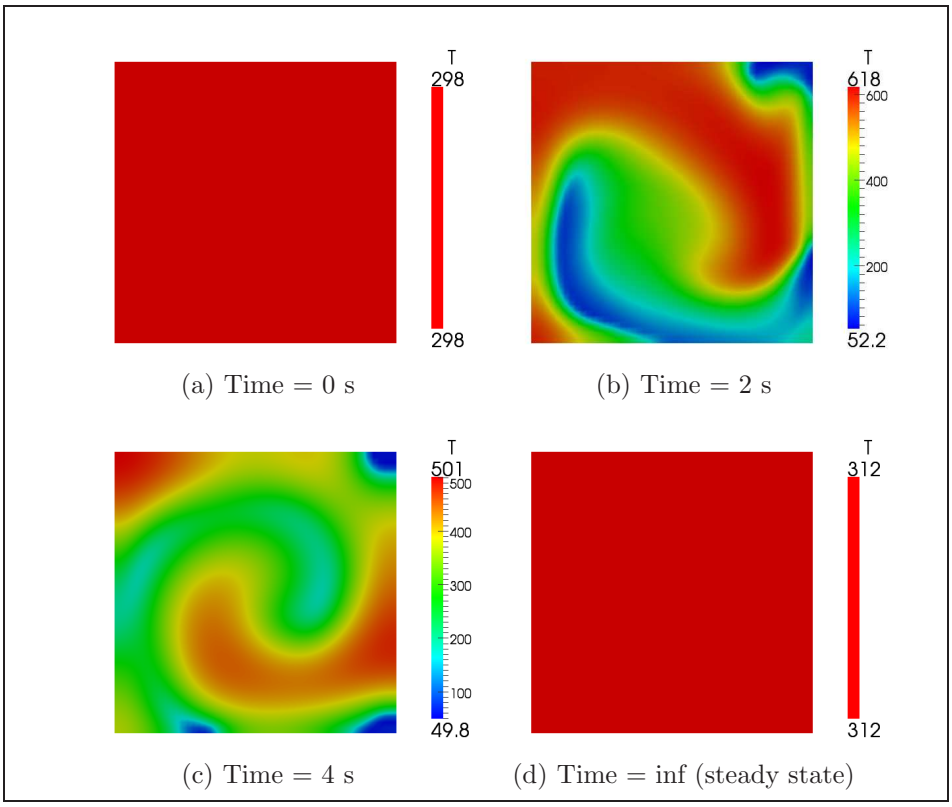

(a) Time = 0 s (b) Time = 2 s

(c) Time = 4 s (d) Time = inf (steady state)

Figure 16: Temperature field (K) in different time steps - mixing box.

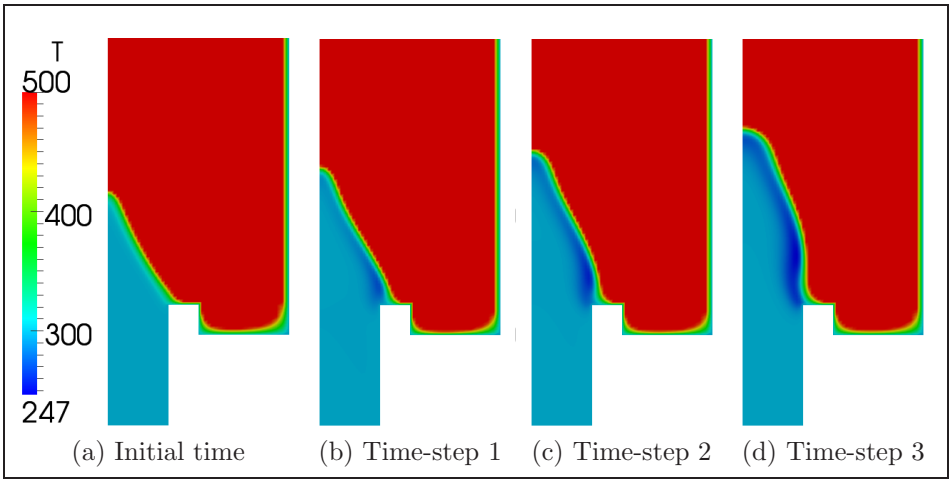

(a) Initial time (b) Time-step 1 (c) Time-step 2 (d) Time-step 3

Figure 17: Temperature field (K) in different time steps - fully premixed case.

gets, the mixture properties. The mixture properties are computed and provided by Cantera. Accessing these properties involves heavy casting and specializing for the

chemistry implementation actually used. Annex .2 shows the procedure to change the enthalpy equation to the Sc=1 assumption in reactingFOAM (OF-1.5).

.2 hEqn.H in OF-1.5 with Sc=1 assumption

The total enthalpy equation with the assumption of a unity Schmidt number reads:

$$\frac{\partial(\rho h)}{\partial t} + \nabla \cdot (\rho \mathbf{u} h) - \nabla \cdot (\alpha \nabla h) = \frac{Dp}{Dt} + \sum_{k=1}^{N_s} \{\nabla \cdot [h_k(\mu - \alpha)] \nabla Y_k\} \tag{3}$$

Therefore in OpenFOAM it becomes:

```
{
  reactingMixture& multiMix = (reactingMixture&) thermo->composition();
  PtrList<reactingMixture::reactionThermo> speciesData = multiMix.speciesData();
  {
    energySource *= 0.0;
    surfaceScalarField alphaF = fvc::interpolate(turbulence->alphaEff() );
    surfaceScalarField muF = fvc::interpolate( turbulence->muEff() );
    volScalarField hY("hY",h);
    surfaceScalarField alphaH("alphaH", alphaF * fvc::interpolate( h) );

    for (label i = 0; i < Y.size(); i++)
    {
     Info <<"\tCalculating differential flux for species" << Y[i].name() << endl;
     reactingMixture::reactionThermo& spData = speciesData[i];
     forAll(T, iCell)
      {
       hY[iCell] = spData.H(T[iCell] );
      }

    alphaH = fvc::interpolate(hY) * (muF - alphaF);
    energySource += fvc::laplacian( alphaH, Y[i] );
    }
  }

  solve
    (
        fvm::ddt(rho, h)
      + mvConvection->fvmDiv(phi, h)
      - fvm::laplacian(turbulence->alphaEff(), h)
     ==
        DpDt
      + energySource
    );
    thermo->correct();
}
```

.3 Chemichal Mechanisms

.3.1 DRM-19

```
!<><><><><><><><><><><><><><><><><><><><><><><><><><><><><><><><><><><><><><><><><<!
!  Reduced version of GRI-MECH 1.2. 19 species ( + N2, AR); 84 reactions. !
!                               PennState Dec, 1994                       !
!<><><><><><><><><><><><><><><><><><><><><><><><><><><><><><><><><><><><><><><><><<!
ELEMENTS
O  H  C  N  AR
END
SPECIES
H2      H       O       O2      OH      H2O     HO2
CH2     CH2(S)  CH3     CH4     CO      CO2     HCO
CH2O    CH3O    C2H4    C2H5    C2H6
N2      AR
END
REACTIONS
O+H+M<=>OH+M                              5.000E+17   -1.000      0.00
H2/2.00/ H2O/6.00/ CH4/2.00/ CO/1.50/ CO2/2.00/ C2H6/3.00/ AR/0.70/
O+H2<=>H+OH                               5.000E+04    2.670   6290.00
O+HO2<=>OH+O2                             2.000E+13    0.000      0.00
O+CH2<=>H+HCO                             8.000E+13    0.000      0.00
O+CH2(S)<=>H+HCO                          1.500E+13    0.000      0.00
O+CH3<=>H+CH2O                            8.430E+13    0.000      0.00
O+CH4<=>OH+CH3                            1.020E+09    1.500   8600.00
O+CO+M<=>CO2+M                            6.020E+14    0.000   3000.00
H2/2.00/ O2/6.00/ H2O/6.00/ CH4/2.00/ CO/1.50/ CO2/3.50/ C2H6/3.00/ AR/0.50/
O+HCO<=>OH+CO                             3.000E+13    0.000      0.00
O+HCO<=>H+CO2                             3.000E+13    0.000      0.00
O+CH2O<=>OH+HCO                           3.900E+13    0.000   3540.00
O+C2H4<=>CH3+HCO                          1.920E+07    1.830    220.00
O+C2H5<=>CH3+CH2O                         1.320E+14    0.000      0.00
O+C2H6<=>OH+C2H5                          8.980E+07    1.920   5690.00
O2+CO<=>O+CO2                             2.500E+12    0.000  47800.00
O2+CH2O<=>HO2+HCO                         1.000E+14    0.000  40000.00
H+O2+M<=>HO2+M                            2.800E+18   -0.860      0.00
O2/0.00/ H2O/0.00/ CO/0.75/ CO2/1.50/ C2H6/1.50/ N2/0.00/ AR/0.00/
H+2O2<=>HO2+O2                            3.000E+20   -1.720      0.00
H+O2+H2O<=>HO2+H2O                        9.380E+18   -0.760      0.00
H+O2+N2<=>HO2+N2                          3.750E+20   -1.720      0.00
H+O2+AR<=>HO2+AR                          7.000E+17   -0.800      0.00
H+O2<=>O+OH                               8.300E+13    0.000  14413.00
2H+M<=>H2+M                               1.000E+18   -1.000      0.00
H2/0.00/ H2O/0.00/ CH4/2.00/ CO2/0.00/ C2H6/3.00/ AR/0.63/
2H+H2<=>2H2                               9.000E+16   -0.600      0.00
2H+H2O<=>H2+H2O                           6.000E+19   -1.250      0.00
2H+CO2<=>H2+CO2                           5.500E+20   -2.000      0.00
H+OH+M<=>H2O+M                            2.200E+22   -2.000      0.00
```

```
H2/0.73/ H2O/3.65/ CH4/2.00/ C2H6/3.00/ AR/0.38/
H+HO2<=>O2+H2                           2.800E+13    0.000   1068.00
H+HO2<=>2OH                             1.340E+14    0.000    635.00
H+CH2(+M)<=>CH3(+M)                     2.500E+16   -0.800      0.00
     LOW  /  3.200E+27   -3.140   1230.00/
     TROE/  0.6800   78.00  1995.00  5590.00 /
H2/2.00/ H2O/6.00/ CH4/2.00/ CO/1.50/ CO2/2.00/ C2H6/3.00/ AR/0.70/
H+CH3(+M)<=>CH4(+M)                     1.270E+16   -0.630    383.00
     LOW  /  2.477E+33   -4.760   2440.00/
     TROE/  0.7830   74.00  2941.00  6964.00 /
H2/2.00/ H2O/6.00/ CH4/2.00/ CO/1.50/ CO2/2.00/ C2H6/3.00/ AR/0.70/
H+CH4<=>CH3+H2                          6.600E+08    1.620  10840.00
H+HCO(+M)<=>CH2O(+M)                    1.090E+12    0.480   -260.00
     LOW  /  1.350E+24   -2.570   1425.00/
     TROE/  0.7824  271.00  2755.00  6570.00 /
H2/2.00/ H2O/6.00/ CH4/2.00/ CO/1.50/ CO2/2.00/ C2H6/3.00/ AR/0.70/
H+HCO<=>H2+CO                           7.340E+13    0.000      0.00
H+CH2O(+M)<=>CH3O(+M)                   5.400E+11    0.454   2600.00
     LOW  /  2.200E+30   -4.800   5560.00/
     TROE/  0.7580   94.00  1555.00  4200.00 /
H2/2.00/ H2O/6.00/ CH4/2.00/ CO/1.50/ CO2/2.00/ C2H6/3.00/
H+CH2O<=>HCO+H2                         2.300E+10    1.050   3275.00
H+CH3O<=>OH+CH3                         3.200E+13    0.000      0.00
H+C2H4(+M)<=>C2H5(+M)                   1.080E+12    0.454   1820.00
     LOW  /  1.200E+42   -7.620   6970.00/
     TROE/  0.9753  210.00   984.00  4374.00 /
H2/2.00/ H2O/6.00/ CH4/2.00/ CO/1.50/ CO2/2.00/ C2H6/3.00/ AR/0.70/
H+C2H5(+M)<=>C2H6(+M)                   5.210E+17   -0.990   1580.00
     LOW  /  1.990E+41   -7.080   6685.00/
     TROE/  0.8422  125.00  2219.00  6882.00 /
H2/2.00/ H2O/6.00/ CH4/2.00/ CO/1.50/ CO2/2.00/ C2H6/3.00/ AR/0.70/
H+C2H6<=>C2H5+H2                        1.150E+08    1.900   7530.00
H2+CO(+M)<=>CH2O(+M)                    4.300E+07    1.500  79600.00
     LOW  /  5.070E+27   -3.420  84350.00/
     TROE/  0.9320  197.00  1540.00 10300.00 /
H2/2.00/ H2O/6.00/ CH4/2.00/ CO/1.50/ CO2/2.00/ C2H6/3.00/ AR/0.70/
OH+H2<=>H+H2O                           2.160E+08    1.510   3430.00
2OH<=>O+H2O                             3.570E+04    2.400  -2110.00
OH+HO2<=>O2+H2O                         2.900E+13    0.000   -500.00
OH+CH2<=>H+CH2O                         2.000E+13    0.000      0.00
OH+CH2(S)<=>H+CH2O                      3.000E+13    0.000      0.00
OH+CH3<=>CH2+H2O                        5.600E+07    1.600   5420.00
OH+CH3<=>CH2(S)+H2O                     2.501E+13    0.000      0.00
OH+CH4<=>CH3+H2O                        1.000E+08    1.600   3120.00
OH+CO<=>H+CO2                           4.760E+07    1.228     70.00
OH+HCO<=>H2O+CO                         5.000E+13    0.000      0.00
OH+CH2O<=>HCO+H2O                       3.430E+09    1.180   -447.00
OH+C2H6<=>C2H5+H2O                      3.540E+06    2.120    870.00
HO2+CH2<=>OH+CH2O                       2.000E+13    0.000      0.00
```

```
HO2+CH3<=>O2+CH4                          1.000E+12    0.000      0.00
HO2+CH3<=>OH+CH3O                         2.000E+13    0.000      0.00
HO2+CO<=>OH+CO2                           1.500E+14    0.000  23600.00
CH2+O2<=>OH+HCO                           1.320E+13    0.000   1500.00
CH2+H2<=>H+CH3                            5.000E+05    2.000   7230.00
CH2+CH3<=>H+C2H4                          4.000E+13    0.000      0.00
CH2+CH4<=>2CH3                            2.460E+06    2.000   8270.00
CH2(S)+N2<=>CH2+N2                        1.500E+13    0.000    600.00
CH2(S)+AR<=>CH2+AR                        9.000E+12    0.000    600.00
CH2(S)+O2<=>H+OH+CO                       2.800E+13    0.000      0.00
CH2(S)+O2<=>CO+H2O                        1.200E+13    0.000      0.00
CH2(S)+H2<=>CH3+H                         7.000E+13    0.000      0.00
CH2(S)+H2O<=>CH2+H2O                      3.000E+13    0.000      0.00
CH2(S)+CH3<=>H+C2H4                       1.200E+13    0.000   -570.00
CH2(S)+CH4<=>2CH3                         1.600E+13    0.000   -570.00
CH2(S)+CO<=>CH2+CO                        9.000E+12    0.000      0.00
CH2(S)+CO2<=>CH2+CO2                      7.000E+12    0.000      0.00
CH2(S)+CO2<=>CO+CH2O                      1.400E+13    0.000      0.00
CH3+O2<=>O+CH3O                           2.675E+13    0.000  28800.00
CH3+O2<=>OH+CH2O                          3.600E+10    0.000   8940.00
2CH3(+M)<=>C2H6(+M)                       2.120E+16   -0.970    620.00
     LOW  /  1.770E+50   -9.670   6220.00/
     TROE/  0.5325  151.00  1038.00  4970.00 /
H2/2.00/ H2O/6.00/ CH4/2.00/ CO/1.50/ CO2/2.00/ C2H6/3.00/ AR/0.70/
2CH3<=>H+C2H5                             4.990E+12    0.100  10600.00
CH3+HCO<=>CH4+CO                          2.648E+13    0.000      0.00
CH3+CH2O<=>HCO+CH4                        3.320E+03    2.810   5860.00
CH3+C2H6<=>C2H5+CH4                       6.140E+06    1.740  10450.00
HCO+H2O<=>H+CO+H2O                        2.244E+18   -1.000  17000.00
HCO+M<=>H+CO+M                            1.870E+17   -1.000  17000.00
H2/2.00/ H2O/0.00/ CH4/2.00/ CO/1.50/ CO2/2.00/ C2H6/3.00/
HCO+O2<=>HO2+CO                           7.600E+12    0.000    400.00
CH3O+O2<=>HO2+CH2O                        4.280E-13    7.600  -3530.00
C2H5+O2<=>HO2+C2H4                        8.400E+11    0.000   3875.00
END
```

Bibliography

[1] A.Prochilo *Development and validation of an incompressible transient laminar-combustion solver in OpenFOAM* ,Master, thesis, Politecnico di Torino - UIC, 2009.

[2] B.Fiorina, R.Baron, O.Gicquel, D.Thevenin, S.Carpentier, and N.Darabiha. (2003) *Modelling non-adiabaticpartially premixed flames using flame-prolongation of ILDM*, Combustion Theory and Modelling, 7:3, 449-470.

[3] N.Peters. *Turbulent Combustion*, Cambridge University Press, Cambridge, 2000.

[4] Forman A.Williams *Combustion Theory*, Benjamin/Cummins, Menlo Park, CA, 1985

[5] Altimira, K. C., 2005, *Numerical Simulation of Non-premixed Laminar and Turbulent Flames by means of Flamelet Modelling Approaches*, Ph.D. Dissertation, Polytechnic University of Catalonia, Barcelona, Spain.

[6] Poinsot, T., and Veynante, D., 2005, *Theoretical and Numerical Combustion*, Second Edition, R.T. Edwards, USA.

[7] Kuo, K. K., 2005, *Principles of Combustion, Second Edition*, John Wiley & Sons, USA.

[8] V.Rivola, *Comparative Study of the CFD code Mistral and OpenFOAM*, Thesis, France, 2007

[9] T.Poinsot, D.Veynante, *Theoretical and Numerical Combistion*, second edition, Edwards, 2005

[10] Chung K.Law, *Combustion Physics* Cambridge University Press, 2006

[11] OpenFOAM user guide, 2009

[12] `http://openfoamwiki.net/index.php/Contrib_groovyBC`

[13] `http://www.me.berkeley.edu/drm/drm19.dat`

[14] F.P.Karrholm *Numerical Modelling of Diesel Spray Injection, Turbulence Interaction and Combustion*, phd thesis, Chalmers University of Technology,Goteborg, Sweden, 2008

[15] R.D.Gould, W.H.stevenson, H.D.Thompson, *Simulation Velocity and Temperature Measurements in a Premixed Dump Combustor*, Journal of Propulsion and Power, Vol.10, No. 5, sept-Oct 1994

[16] H. Kanchi, K. Russell, K. Sengupta, F. Mashayek, *Fluidic control of reacting flow using microjets in an axisymmetric dump combustor* University of Illinois at Chicago, Chicago, IL 60607, USA.

[17] `http://openfoamwiki.net/index.php/HowTo_Using_the_WaveTransmissive_Boundary_`

[18] `http://code.google.com/p/cantera/`

[19] `http://groups.google.com/group/cantera-users`

[20] `http://my.fit.edu/itresources/manuals/fluent6.3/help/html/ug/main_pre.htm`